AD-A083 346 PARTICLE MEASURING SYSTEMS INC BOULDER COLO F/G 19/4
RESULTS OF THE MISERS BLUFF II AIRCRAFT DUST PARTICLE SAMPLING --ETC(U)
MAY 79 R G KNOLLENBERG DNA001-78-C-0232

UNCLASSIFIED DNA-4951F NL

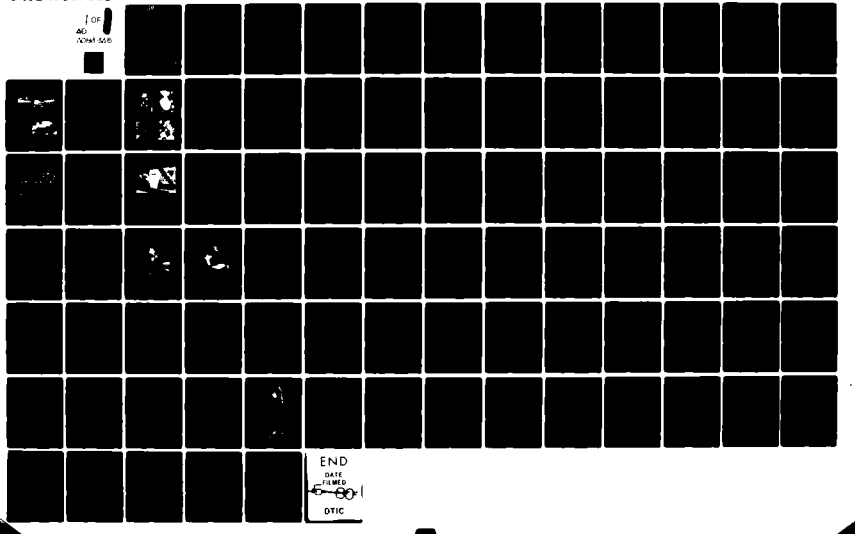

END
DATE FILMED
DTIC

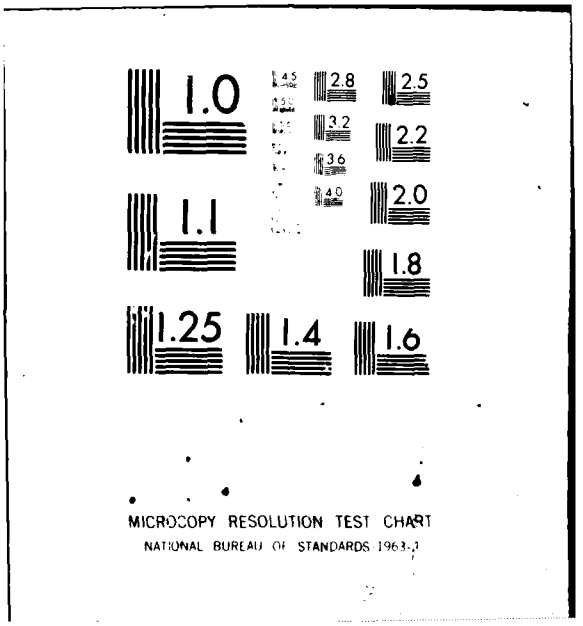
1.0
1.1
1.25
1.4
1.6
1.8
2.0
2.2
2.5
2.8
3.2
3.6
4.0
MICROCOPY RESOLUTION TEST CHART
NATIONAL BUREAU OF STANDARDS 1963-A

DNA 4951F

RESULTS OF THE MISERS BLUFF II AIRCRAFT DUST PARTICLE SAMPLING EXPERIMENTS

Robert G. Knollenberg
Particle Measuring Systems , Inc.
1855 South 57th Court
Boulder, Colorado 80301

30 May 1979

Final Report for Period 1 May 1978—30 May 1979

CONTRACT No. DNA 001-78-C-0232

APPROVED FOR PUBLIC RELEASE;
DISTRIBUTION UNLIMITED.

THIS WORK SPONSORED BY THE DEFENSE NUCLEAR AGENCY
UNDER RDT&E RMSS CODES B342078462 H35HAXYX95603 H2590D
AND X342078469 Q78HAXYX95601 H2590D.

Prepared for
Director
DEFENSE NUCLEAR AGENCY
Washington, D. C. 20305

Destroy this report when it is no longer needed. Do not return to sender.

PLEASE NOTIFY THE DEFENSE NUCLEAR AGENCY, ATTN: STTI, WASHINGTON, D.C. 20305, IF YOUR ADDRESS IS INCORRECT, IF YOU WISH TO BE DELETED FROM THE DISTRIBUTION LIST, OR IF THE ADDRESSEE IS NO LONGER EMPLOYED BY YOUR ORGANIZATION.

UNCLASSIFIED

SECURITY CLASSIFICATION OF THIS PAGE *(When Data Entered)*

REPORT DOCUMENTATION PAGE	READ INSTRUCTIONS BEFORE COMPLETING FORM
1. REPORT NUMBER: DNA 4951F / 2. GOVT ACCESSION NO.: AD-A083 346	3. RECIPIENT'S CATALOG NUMBER
4. TITLE *(and Subtitle)*: RESULTS OF THE MISERS BLUFF II AIRCRAFT DUST PARTICLE SAMPLING EXPERIMENTS	5. TYPE OF REPORT & PERIOD COVERED: Final Report for Period 1 May 1978—30 May 1979
	6. PERFORMING ORG. REPORT NUMBER
7. AUTHOR(s): Dr. Robert G. Knollenberg	8. CONTRACT OR GRANT NUMBER(s): DNA 001-78-C-0232 new
9. PERFORMING ORGANIZATION NAME AND ADDRESS: Particle Measuring Systems, Inc. 1855 South 57th Court Boulder, Colorado 80301	10. PROGRAM ELEMENT, PROJECT, TASK AREA & WORK UNIT NUMBERS: Subtasks H35HAXYX956-03 and Q78HAXYX956-01
11. CONTROLLING OFFICE NAME AND ADDRESS: Director Defense Nuclear Agency Washington, D.C. 20305	12. REPORT DATE: 30 May 1979
	13. NUMBER OF PAGES: 86
14. MONITORING AGENCY NAME & ADDRESS*(if different from Controlling Office)*	15. SECURITY CLASS *(of this report)*: UNCLASSIFIED
	15a. DECLASSIFICATION DOWNGRADING SCHEDULE

16. DISTRIBUTION STATEMENT *(of this Report)*

Approved for public release; distribution unlimited.

17. DISTRIBUTION STATEMENT *(of the abstract entered in Block 20, if different from Report)*

18. SUPPLEMENTARY NOTES

This work sponsored by the Defense Nuclear Agency under RDT&E RMSS Codes B342078462 H35HAXYX95603 H2590D and X342078469 Q78HAXYX95601 H2590D.

19. KEY WORDS *(Continue on reverse side if necessary and identify by block number)*

High Explosive Generated Dust Clouds
Particle Size Distribution
Airborne Dust Measurements
Mass Loading, Extinction Coefficients
Optical Particle Sizing
Misers Bluff II

20. ABSTRACT *(Continue on reverse side if necessary and identify by block number)*

Dust clouds generated from two high explosive detonations of 100 and 600 tons (TNT equivalent) in the Misers Bluff II Experiment were sampled with an instrumented aircraft to determine the size and number density of particulates from 0.1 to 10,000 μm. The primary sizing techniques utilized "in situ" optical methodology. High resolution dust concentration measurements were performed from approximately T + 3 to T + 60 minutes

DD FORM 1 JAN 73 1473 EDITION OF 1 NOV 65 IS OBSOLETE

UNCLASSIFIED

SECURITY CLASSIFICATION OF THIS PAGE *(When Data Entered)*

20. ABSTRACT (Continued)

during both experiments. The total mass lofted integrated from these samples was found to be 0.80 x 10^9gm and 5.23 x 10^9gm for the experiment pair. Typical mass loadings were a few tenths of a gram per cubic meter. Visibilities to less than 100 meters were encountered with single pass optical depths 10-45 in the well developed cloud regions. The largest dust particles observed were only about 2 mm diameter. Organic particles up to 10 mm long are widely dispersed with the dust particles. Mean mass sizes of 90-160 μm are typical. Turbulence was light at even the earliest passes. Aircraft damage was restricted to injected dirt creating small but measurable engine wear.

TABLE OF CONTENTS

LIST OF FIGURES

List of Figures (con't)

LIST OF TABLES

1.0 INTRODUCTION

Various studies of dust clouds generated by high explosives (HE) have been performed sporadically over the past ten years (1 & 2). Several of the studies have involved aircraft samplings of the particulates lofted by these surface blasts. The primary sampling methods employed by these various aircraft have been impactors, filters, cyclones and other direct collection devices. To a large degree these were the best, if not only, tools available for such tasks at the time. However, during the last few years, a significant improvement in capabilities for airborne particle sizing has been afforded in *in situ* optical particle size spectrometers (3 & 4). These aircraft mounted devices largely developed by Particle Measuring Systems, Inc. (hereafter PMS) embody light scattering and imaging principles to cover sizes from 0.1 to 10,000 μm. These instruments have become the primary measurement tools of scientists currently involved in experimental cloud physics research.

The MISERS BLUFF II HE experiments on 28 June and 30 August, 1978 provided the first opportunity to engage this type of technology to quantify and detail the microstructure of such HE generated dust clouds. PMS fielded an instrumented Cessna 206 aircraft for the MISERS BLUFF II experiments to perform *in situ* particle size spectrometry in the 0.1 to 10,000 μm range. Other measurements included state parameters and video recorded imagery of each cloud pass. This field effort involved a complete experimental program requiring experiment design, aircraft instrumentation, calibrations, operations, and data collection and analysis.

The size and spatial resolution obtained were sufficient to generate independent size spectra for every few tens to hundreds of meters of flight path with still higher flight path (time) resolution for particles larger than 5.0 μm and particle morphological data on a particle-by-particle basis for particles larger than ∿100 μm. The importance of obtaining this high resolution particle size distribution information during the MISERS BLUFF II experiments contributes not only to information

on the detailed microstructure but also to the more complete determination of the total mass budget of the dust clouds. The microstructural data will aid the interpretation of microwave and optical experiments (DNA/RAAE). Integrated mass loadings from a stacked vertical array of cloud pass samples from both experiments will provide the inputs to validate superposition theories postulated for scaling multiburst mass loading (to be published by Science Applications, Inc.DNA Control #001-78-C-0217).

The MISERS BLUFF II series were conducted at the Planet Ranch Test site near Lake Havasu City, Arizona. The first event in the MISERS BLUFF II series (MISERS BLUFF II-1) was the detonation of a single 120 ton ANFO* charge (100 ton TNT equivalent) on 28 June 1978. Six identical 120 ton ANFO charges (600 ton TNT or 1.2 kt nuclear blast equivalent) were simultaneously detonated on 30 August 1978 (MISERS BLUFF II-2). They were set on a hexagonal array with a 200 meter diameter within 1330 feet of the first crater in the Bill Williams riverbed.

The PMS Cessna 206 research aircraft initiated direct penetrations in the dust cloud lofted by both explosions within 2-5 minutes after detonation. While the research payload and performance varied slightly between MISERS BLUFF II-1 and MISERS BLUFF II-2, the important optical and mass properties of both cloud systems were adequately sampled with approximately 20 sampling penetrations in both experiments.

These airborne sampling experiments were part of an integrated set of experiments involving ground and remote sampling as well as direct *in situ* measurements. This report describes the work PMS undertook in the airborne *in situ* measurements. The next section describes the instrument payload and field operations followed by the results of MISERS BLUFF II-1 and MISERS BLUFF II-2. A discussion of the results is included followed by the conclusions reached and suggestions for further data processing and analysis.

Finally, this report presents only a small sample of

*∿94% Ammonium Nitrate with ∿6% Fuel Oil.

the total data collected. It is not an attempt to thoroughly analyze the data in detail. Rather it describes typical results and an integrated picture of the particulates which characterize these HE generated dust clouds. Further analysis is being conducted by others and will be reported in the future.

2.0 EXPERIMENT DESCRIPTION

PMS provided DNA with a completely calibrated airborne particle spectrometer measurement platform capable of measuring the size distribution of particulates in HE generated MISERS BLUFF II dust clouds for a field period of four weeks, operated and gathered data with this system, and performed preliminary analysis of the data obtained. Calibrations were performed at PMS using a Calibration Wind Tunnel Facility before delivery of the system to MISERS BLUFF and after its return. Initial data analysis conducted at PMS after the post-calibration check utilized existing software analysis routines. More detailed analyses were performed in the months following the field efforts and are described in Section 3.0.

2.1 The PMS Cessna 206 Research Aircraft

The PMS Cessna 206 Aircraft (hereafter PMS 206) was primarily designed as a testbed for various PMS spectrometers. As such, it was modified with sufficient hard points established to simultaneously carry four PMS *in situ* particle size spectrometers (Fig. 2.1) and a fifth plumbed aerosol device for MISERS BLUFF II-2. This gives the aircraft complete coverage of the *in situ* dynamic range available. Even with its full payload of instrumentation, the aircraft has good performance --- especially for an air sampling aircraft. Its relatively low sampling airspeed envelope coupled with standard utility category stress loadings give it the same margin of safety in turbulence as a higher stressed aircraft sampling at high airspeed.

2.2 PMS Cessna 206 Instrument Payload for MISERS BLUFF Experiments

Of particular importance to this program was the PMS 206's ability to carry the four external spectrometer probes as shown in Fig. 2.1. This group of instruments included:

1 Forward Scattering Spectrometer Probe Model FSSP-100 Size Range: 0.5 - 47 μm

Above: Photograph of PMS 206 Research Aircraft at Lake Havasu City, Arizona airport taken before MISERS BLUFF II-2.

Right: Close up of wing tip installation of OAP-200X and FSSP-100 probes. Note the horizontal orientation of the OAP-200X and the Rosemount temperature probe installed on the back hemisphere of the FSSP.

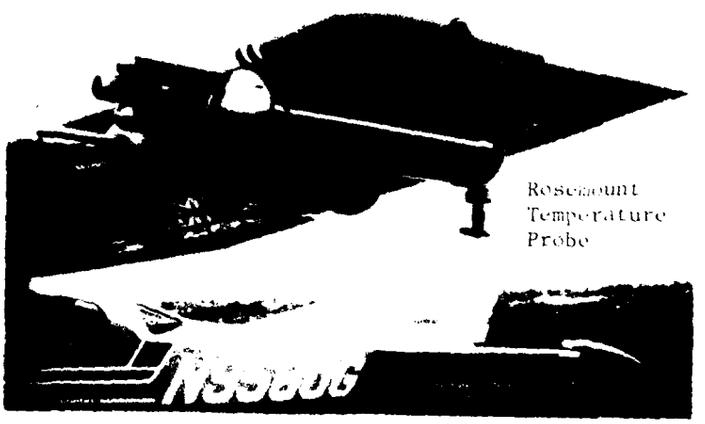

Figure 2.1. PMS 206 Research Aircraft

1	Optical Array Cloud Droplet Probe Model OAP-200X	Size Range: 20 - 300 μm
2	Optical Array Spectrometer Probes Models OAP-2D-C and OAP-2D-P	Size Ranges: 25 - 6,000 μm

This selection of probes was made after reviewing reports on previous measurements and analysis of soil samples from the Ground Zero area at the Planet Ranch test site. PMS personnel took soil samples of the area on the 2 March 1978 site visit. Surface samples as well as core samples were integrated and then analyzed at PMS. The soil was typically fine sandy alluvial deposits with a few large rocks. The best estimate of what could be lofted during the pair of tests was made from the analysis of these sandy soil samples. The soil samples indicated the following bulk properties:

% Fines (<16 mesh):	83.9%
% Aggregate (>16 mesh):	16.1%
Fines bulk density:	1.34 gm cm^{-3}
Aggregate bulk density:	1.62 gm cm^{-3}
Fines average mineral density:	2.29 gm cm^{-3}
Aggregate average mineral density:	2.59 gm cm^{-3}
Mineral types:	Mica, shists, silica and granitic rock

Photomicrographs of the fines are given in Fig. 2.2. Size and mass distribution measurements were made with a 2D probe (25 μm resolution) of the fines and are presented in Fig. 2.3 and 2.4. Particles larger than 650 μm are absent in this sample because of the finite size of the sample (13,841) and the low sample probability at the larger sizes providing an excellent demonstration of the importance of the OAP-2D-P (hereafter 2D-P) instrument for the actual MISERS BLUFF II tests. Even with the lack of the measurements at the larger sizes it is clear that the mass would be expected to peak out at sizes of 200 to 300 μm or less.

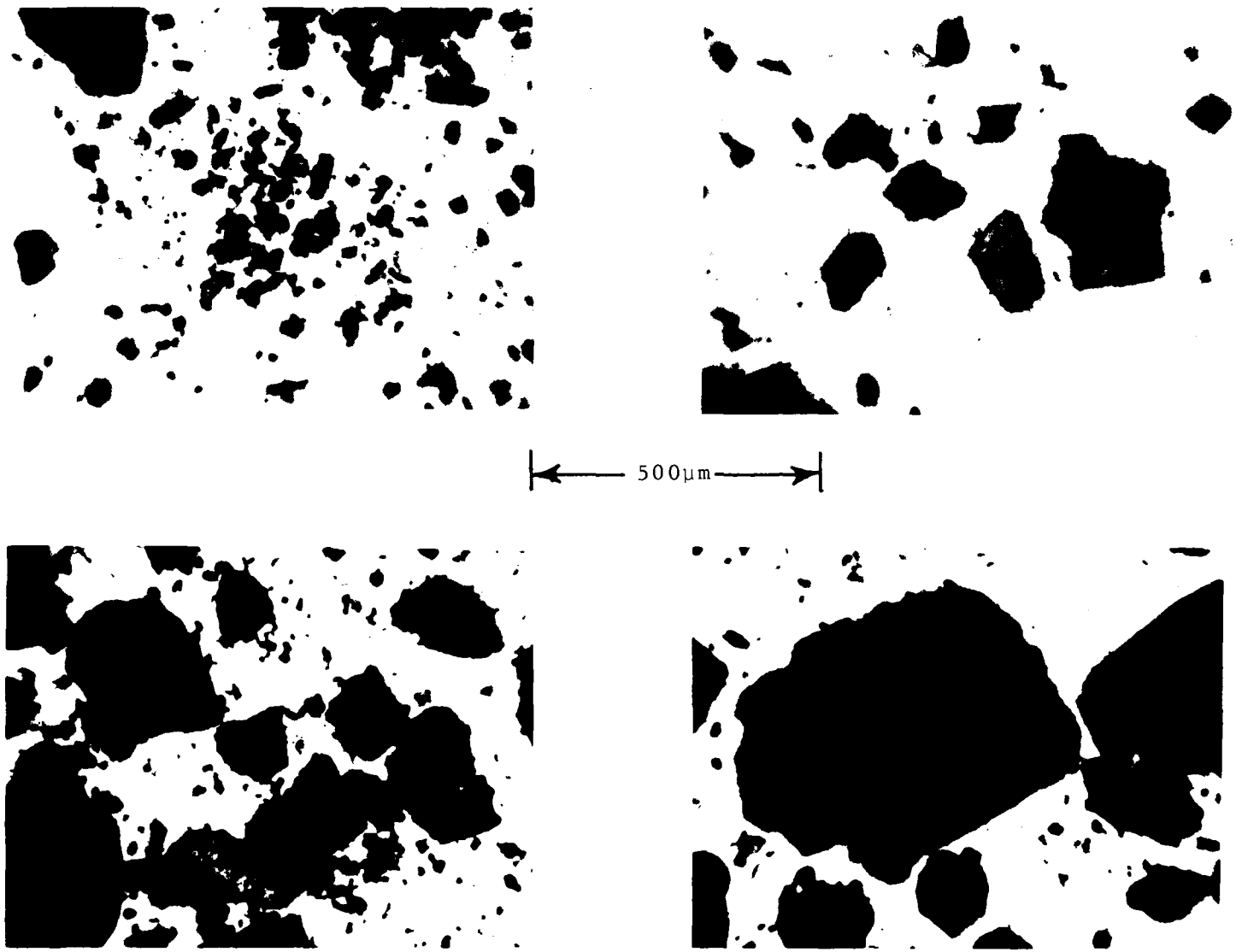

Fig. 2.2: Photomicrographs of soil samples from Ground Zero, MISERS BLUFF

SIZE DISTRIBUTION FROM SOIL SAMPLES AT GROUND ZERO MISERS BLUFF II

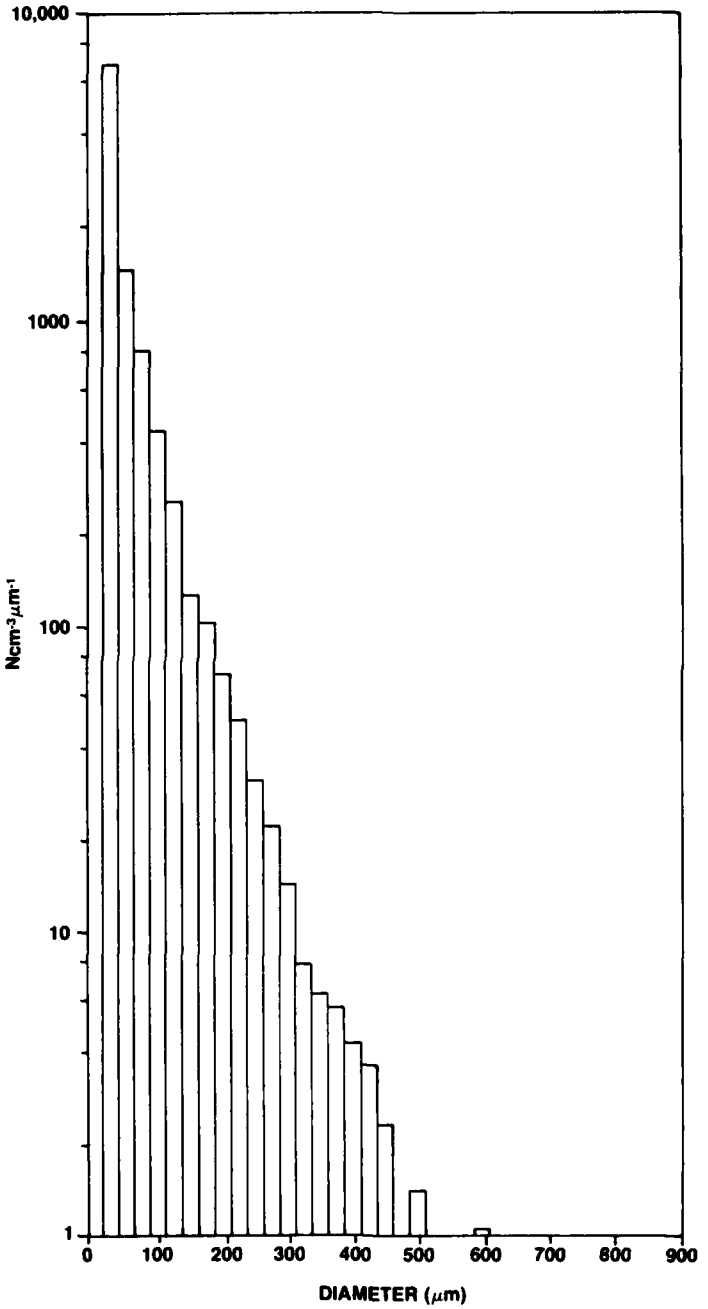

Figure 2.3: The size distribution of the soil samples taken at Ground Zero, MISERS BLUFF shows the particle sizes to be rather steeply exponentially distributed. While 13,841 particles were sized there is still insufficient sample to cover the sparce particle sizes greater than 450 μm.

MASS DISTRIBUTION FROM SOIL SAMPLES AT GROUND ZERO MISERS BLUFF II

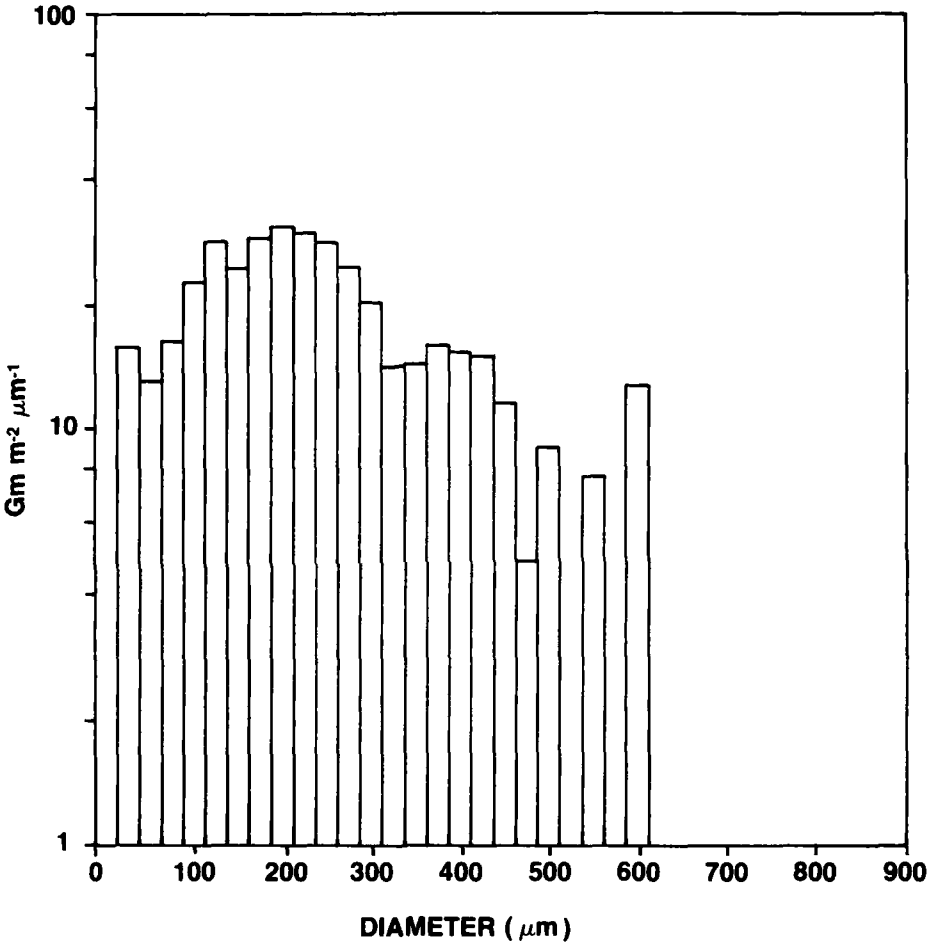

Figure 2.4: The mass distribution above shows a dominant mode at about 200 μm. A secondary mode near 400 μm is also evident. The population sampled is too limited at sizes greater than 450 μm.

After the MISERS BLUFF II-1 data were reduced, a fifth instrument was added to the PMS 206 payload to cover the aerosol subrange below 3 μm diameter. This instrument was a Laser Aerosol Spectrometer Model LAS-X which had a size range of 0.12 to 6.0 μm. Because data system limits allowed for only four probes the LAS-X was time shared with the OAP-200X (hereafter 200X). Table 2.1 summarizes the entire experiment payload for both MISERS BLUFF II-1 and MISERS BLUFF II-2. Descriptions of the spectrometers, state parameter sensors, data acquisition system and the color vidicon imagery system completing this entire instrument payload are detailed below.

2.2.1 Particle Size Spectrometers

The PMS spectrometer probes used at MISERS BLUFF listed in Table 2.1 are further elaborated upon in Table 2.2. The standard size ranges and calibrated size ranges used at MISERS BLUFF require some explanation. The standard size ranges can be adjusted over a factor of two in the optical array instruments that have a zoom movement in their optical imaging system. For instance, in the 200X one can stretch the magnification to 20X to double the resolution to 10 μm if desired. Such changes are possible in the field. However, the 2D-P has a fixed optical system and the magnification is not field adjustable. The Forward Scattering Spectrometer Probe (FSSP) and LAS-X also have fixed size ranges. Standard size ranges were used in MISERS BLUFF II-1 although modified for MISERS BLUFF II-2. This grouping provided a size range coverage from 2.0 μm to above 10,000 μm in MISERS BLUFF II-1. (NOTE: The extension of the 2D-P range must be accomplished through software or manual processing of partial images with corresponding sample areas increasing from 0.1 mm^2 to 1700 mm^2, shown in Fig. 2.5). This sampling format optimized size resolution and sample volume characteristics in the range of approximately a micron to several millimeters. Listed next are detailed descriptions on each of the spectrometers.

INSTRUMENTATION SUMMARY FOR THE PMS 206 RESEARCH AIRCRAFT FOR MISERS BLUFF

Table 2.1

PARAMETER MEASURED	INSTRUMENT TYPE	MANUFACTURER and MODEL NO.	COMBINED PERFORMANCE OF TRANSDUCER, SIGNAL CONDITIONING & RECORDING				
			Range	Accuracy	Time Constant	Precision	Resolution
Temperature	Platinum resistance	Rosemount Eng. Model 102 Probe PMS Transducer	±0.5C	±0.5C	1 sec	0.1C	0.1C
Altitude	Total pressure	National Semi-conductor LX3702A	1000mb	±2mb	1 sec	2mb	0.1mb
IAS	Differential pressure	National Semi-conductor LX3700D	0-3 psid	0.003 psid	1 sec	0.0003 psid	0.0003 psid
Time	Crystal oscillator	Ferwalt, Inc.	12 mo.	±1 sec	NA	NA	1 sec
*Very Small Dust Particles	Laser Aerosol Spectrometer	Particle Measuring Systems LAS-X	0.12-6.0um	0.1um	5 usec	NA	0.1um
Small Dust Particles	Forward Scattering Spectrometer Probe	Particle Measuring Systems FSSP-100	0.5-8.0um 1-16um 2-32um 2-47um	±0.5um ±1um ±2um ±3um	1 usec 1 usec 1 usec 1 usec	NA NA NA NA	0.5um 1um 2um 3um
Small Dust Particles	Optical Array Cloud Droplet	Particle Measuring Systems OAP-200X	10-150um	10um	1/8 usec	NA	10um
Medium Sized Dust Particles	2-D Optical Array Probe	Particle Measuring Systems OAP-2D-C	50-1500um	<50um	1/4 usec	NA	<50um
Large Dust Particles	2-D Optical Array Probe	Particle Measuring Systems OAP-2D-P	200-10,000um	<200um	2 usec	NA	<200um
Data Acquisition System	DAS-2D-32	Particle Measuring Systems DAS-2D-32	NA	NA	NA	NA	200um
Data Recording	Computer Compatible Magnetic Tape	Pertec T7640-9 F649-40	The Pertec Recorder requires 7" computer compatible magnetic tape (600 ft) and provides read-after-write data verification.				

*Misers Bluff II-2 only

Table 2.2

SUMMARY OF SPECTROMETER CHARACTERISTICS FOR MISERS BLUFF

	STANDARD PROBE SAMPLING CHARACTERISTICS				MISERS BLUFF II SAMPLING CHARACTERISTICS		
	Size Range		Sample Area			Calibrated	Calibrated
	Nominal	Calibrated	Nominal	Calibrated		Size Range	Sample Area
FORWARD SCATTERING SPECTROMETER PROBE Model FSSP-100	0.5-45um	0.5-47um	0.3mm^2	0.345mm^2		0.5-47um	0.345mm^2
OPTICAL ARRAY CLOUD DROPLET SPECTROMETER PROBE Model OAP-200X	20-300um	14.2-310um	0.4-17mm^2	0.11-17.08mm^2	MBII-1 MBII-2	24-318um 13-276um	0.11-17.08mm^2 0.13-15.70mm^2
2-D OPTICAL ARRAY SPECTROMETER PROBE Model OAP-2D-C	25-800um	17.5-812.5um	1.25-48mm^2	1.25-48mm^2		17.5-812.5um	1.25-48mm^2
2-D OPTICAL ARRAY SPECTROMETER PROBE Model OAP-2D-P	200-6400um	142-6500um	640-1708.8mm^2	640-1708.8mm^2	MBII-1	142-6500um (142-13,000um)*	640-1708.8mm^2
					MBII-2	70-3100um (70-6200um)*	320-856mm^2
**LAS-X LASER AEROSOL SPECTROMETER	0.12-6.0um	0.12-6.1um	Volume 5cm^{3}sec^{-1}			0.12-6.1um	Volume 5cm^{3}sec^{-1}

*Range extension provided by software routines which determine if particle center lies within array format and processes using 1/2 an image.

**Misers Bluff II-2 only.

SAMPLE AREAS OF SPECTROMETERS USED AT MISERS BLUFF II

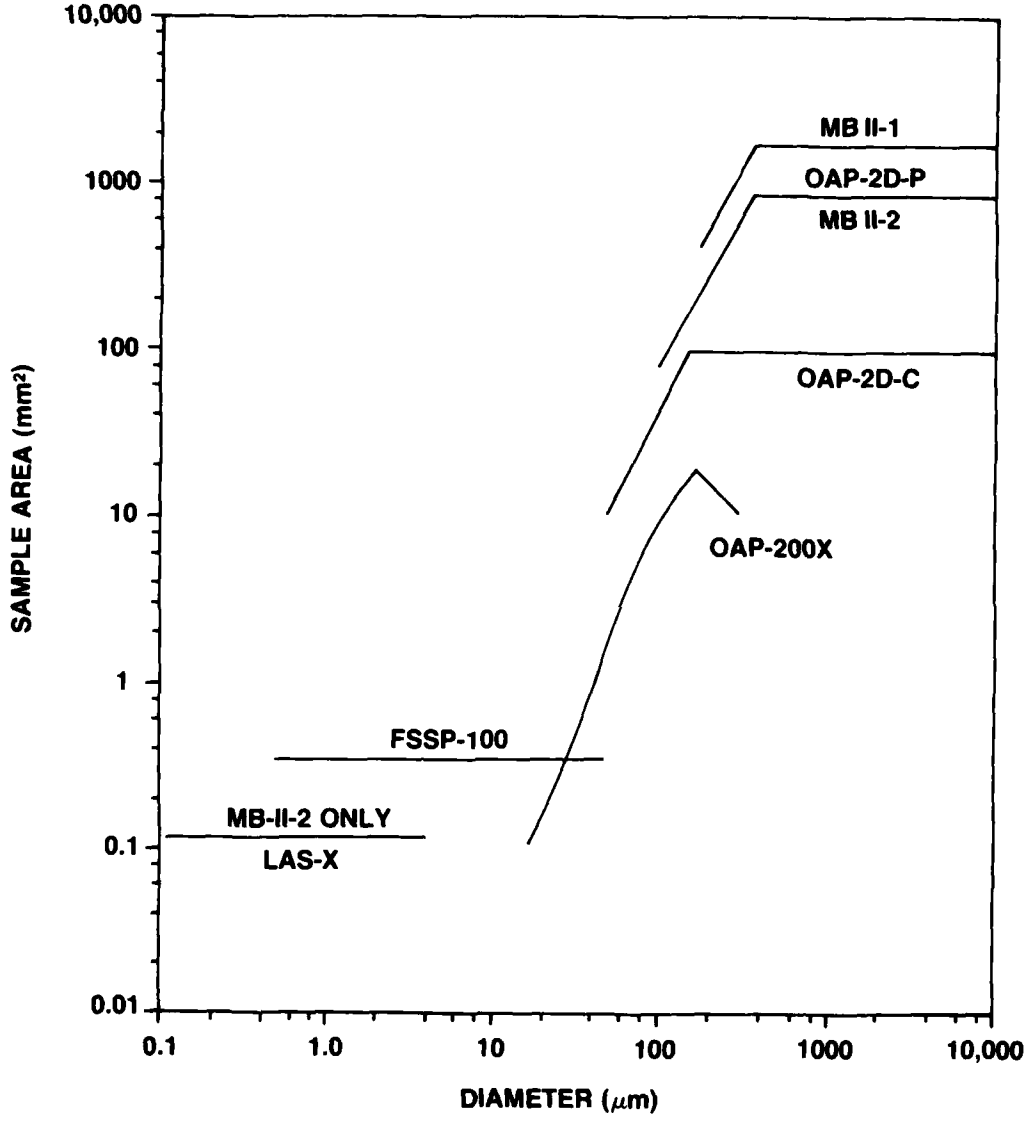

Figure 2.5: The sample areas for the 2D probes shown above are computed assuming partial image analysis is permissible. In fact, most of the data analyses were performed without using this technique resulting in sample areas decreasing with increasing size to the right of the sharp knees in the three top curves. The sample area for the LAS-X is a computed parameter from the constant 5 cm^3 sec^{-1} volumetric flow and an assumed airspeed of 60 m sec^{-1}.

2.2.1.1 Forward Scattering Spectrometer Probe Model FSSP-100

The FSSP is an airborne instrument designed for *in situ* particle size measurements of all types but optimized for water droplets. The FSSP has four overlapping size ranges with each size range divided into fifteen linear size intervals providing up to 60 size channels in the 0.5 to 47 μm range. The FSSP is packaged in a cylindrical pod as a plug-in assembly. Laser and detector alignment is achieved with spring-loaded x-y screw adjustments. The FSSP's He-Ne (632.8 nm) laser tube has an extruded aluminum envelope and is configured in high order multimode. The FSSP pulse height analyzer (PHA) has its reference voltage derived from the source of illumination providing effective automatic gain control (AGC). A programmable amplifier is used to gain switch and provide the size ranging to accommodate the large dynamic range. The probe electronics are self-contained, the output being the particle size in binary code accompanied by a strobe pulse to increment an appropriately addressed memory channel in a data acquisition system (for more detail see Knollenberg [4]).

The single most important feature of the FSSP, increasing its performance, is its high magnification optical system which reduces sample volume to where coincidence errors are less than 10% at concentrations of 10^3 cm^{-3}. For cloud physics work the FSSP normally has a primary size range of 2 to 32 μm diameter, resolving particles into 15 size classes. It is normally set up to size particles having velocities from 10 to 125 m sec^{-1}.

Calibration data for this instrument as configured for MISERS BLUFF II are presented in Table 2.2. The instrument was operated solely in the 2 to 47 μm range.

2.2.1.2 Optical Array Cloud Droplet Spectrometer Probe Model OAP-200X Description

This Optical Array Cloud Droplet Spectrometer Probe is designed to cover a range of 20 to 300 μm. This basic range can be changed by a factor of two using different optics.

The laser used is a He-Ne (632.8 nm) tube of a sealed cavity configuration and of environmental quality.

The optical system includes spherical and cylindrical elements in the condensing optics and spherical elements in the imaging optics with plane dielectric mirror beam folding surfaces. All optical elements are A-R coated for minimal light loss.

The photodiode array is a United Detector Technology device with masked diode elements on 200 μm spacing. The number of active photodiode elements normally used is 24; however, the maximum number of size channels resolved is 15. A Teledyne Philbrick preamplifier is mounted as close as possible to each of the photodiode elements.

The photodetector modules provide a second Teledyne Philbrick amplifier. The two-stage amplifier is added assurance of sufficient light level for severe environment operation. The photodetector modules discriminate the shadowing events of the individual photodiode elements and provide the appropriate logic output signals including a buffer memory. The modules are designed to operate over at least an order of magnitude variation in light level.

The necessary logic to determine the number of photodiodes occulted during a particle shadow transit includes circuitry to make a conversion of unity weighted events to a binary encoded particle size and to reject particles as nonvalid if they are only partially within the designated sample area or are too large to be within the size range of the probe. Additional circuitry includes logic to channel the particle size information out to the data acquisition system and reset the input buffer memory on the photodetector modules.

Calibration data for this instrument as configured for MISERS BLUFF II are presented in Table 2.2 This instrument was used as a back-up for the OAP-2D-C (hereafter 2D-C) instrument described below. Its slightly different calibration characteristics for MISERS BLUFF II-1 vs MISERS BLUFF II-2 arise from the

use of an older type photodiode array in MISERS BLUFF II-1 which had rectangular rather than round elements. This array was changed between experiments to the round element device.

2.2.1.3 Two-Dimensional Optical Array Imaging Probes Models OAP-2D-C and OAP-2D-P

The 2D Particle Imaging Probes utilize a photodiode array and photodetection electronics similar to the standard PMS Optical Array Probes. However, the instruments contain high speed front end data storage registers which enable each photodetector element to transmit up to 1024 bits of shadow information rather than 1 bit of shadow information from each particle. The particle's transit allows the array to scan the particle and *image slices* are recorded across the shadow to develop a true two-dimensional image.

These probes are packaged in cylindrical pods and interface only with a standard PMS Data Acquisition System Model DAS-2D. The probes can collect particle image information at the rate of 128 million bits per second. However, data is recorded only when particles are present and thus, automatic data compression results. The particle information is recorded directly on computer compatible magnetic tape recorders via the DAS-2D. Software has been developed to classify the particles, perform mass computations, or compute various integrated particle parameters as desired from the raw image data via a computer.

The technique employed to achieve 2D information from particles passing through the instrument is to take *image slices* of the particle as it progresses through the sampling volume of a single linear photodiode array. The instrument employs 32 photodiode elements in the array and takes *image slices* at a rate up to 4 million per second when a particle passes through. At a true airspeed of 100m sec^{-1}250 nsec corresponds to 25 μm of motion which is the apparent diameter of each element in the array when the 2D-C probe is calibrated to its nominal calibration of 25 to 800 μm (the lower resolution of the 2D-P instrument has correspondingly coarser resolution and lower slice rate). At this

airspeed, the size resolution across the array (particle width) is identical to the *image slice* resolution through the array (particle length) if a slice rate of 4 MHz is employed. The slice rate can be slaved to true airspeed (TAS) to provide square raw image data at all speeds up to the maximum.

The data from each *image slice* are stored in static MOS shift registers which serve as a buffer for writing onto the computer tape. Actually, two MOS buffers are employed in a *ping-pong* (alternate usage) fashion such that one can be available for loading (at a rate determined by incoming particles) while the other is used to unload a previous sampling of particles (at a rate necessary for proper writing). As long as unloading is accomplished earlier than loading in each case, no *indigestion* is encountered and the buffer roles can be alternately reversed with no loss of data.

The maximum data rate is determined by the tape recorder employed. With a 25 ips machine using 1600 cpi density, the maximum sustained *image slice* rate is about 7K slices per second. A 7 inch reel of tape will last about 5 minutes at this rate, but since image data is recorded only when particles are encountered, the actual recording time per reel will be much longer for typical particle concentrations. The DAS-2D will record on two tape recorders alternately to allow indefinite uninterrupted sampling.

The laser used is a He-Ne (632.8 nm) of a sealed cavity configuration and of environmental quality.

The optical system includes spherical and cylindrical elements in the condensing optics and spherical elements in the imaging optics with plane dielectric mirror beam folding surfaces. All optical elements are A-R coated for minimal light loss.

The photodiode array is a United Detector Technology device with masked circular diode elements on 200 μm spacing. A Teledyne Philbrick preamplifier is mounted as close as possible to each of the photodiode elements.

The photodetector modules provide a second Teledyne Philbrick amplifier. The two stage amplifier is added assurance of sufficient light level for severe environment operation. The

photodetector modules discriminate the shadowing events of the individual photodiode elements and provide the appropriate logic output signals to MOS shift registers. The MOS registers of all photodetector modules are clocked in parallel to store *image slices*.

The necessary logic to clock the MOS registers during load and unload cycles is contained within the probe. A counter also measures the time between particles which is encoded into the particle MOS registers after each particle shadow. Fig. 2.6 shows typical imagery from 2D probes in rain, snow, and the soil samples of Fig. 2.3 and 2.4.

Calibration data for the pair of 2D probes used at MISERS BLUFF II are given in Table 2.2.

2.2.1.4 Laser Aerosol Spectrometer Model LAS-X

The Laser Aerosol Spectrometer, Model LAS-X is an aerosol spectrometer designed for general laboratory use. A single range with sixteen different size classes is used to cover a size range of 0.1 μm to 6.1 μm and greater. Size classes 1 through 15 are used to cover 0.1 μm to 6.1 μm, while size class 16 is greater than 6.1 μm. The LAS-X is a complete laser aerosol spectrometer system and has a built-in printer to provide automatic data logging of particle size spectra.

The laser used is a hybrid 2 mW He-Ne (632.8 nm) unit with TEM_{oo} mode.

The optical system includes two mirrors (one parabolic and one flat at 45°) and one aspheric lens. The parabola has a 5 mm focal length and the asphere has 25 mm focal length. The asphere is A-R coated for minimal light loss. The parabola has a gold reflective coating with approximately 90% reflectivity. The flat mirror has a dielectric coating with 99.0+% reflectivity.

To cover the large dynamic signal output with one range, the preamp section has three outputs with different gain ratios. Each of the outputs inputs to preselected channels of the PHA. The number of channels selected for a given output depends on the slope of the signal strength versus size curve for the particular size range covered.

SAMPLES OF 2D PROBE IMAGERY

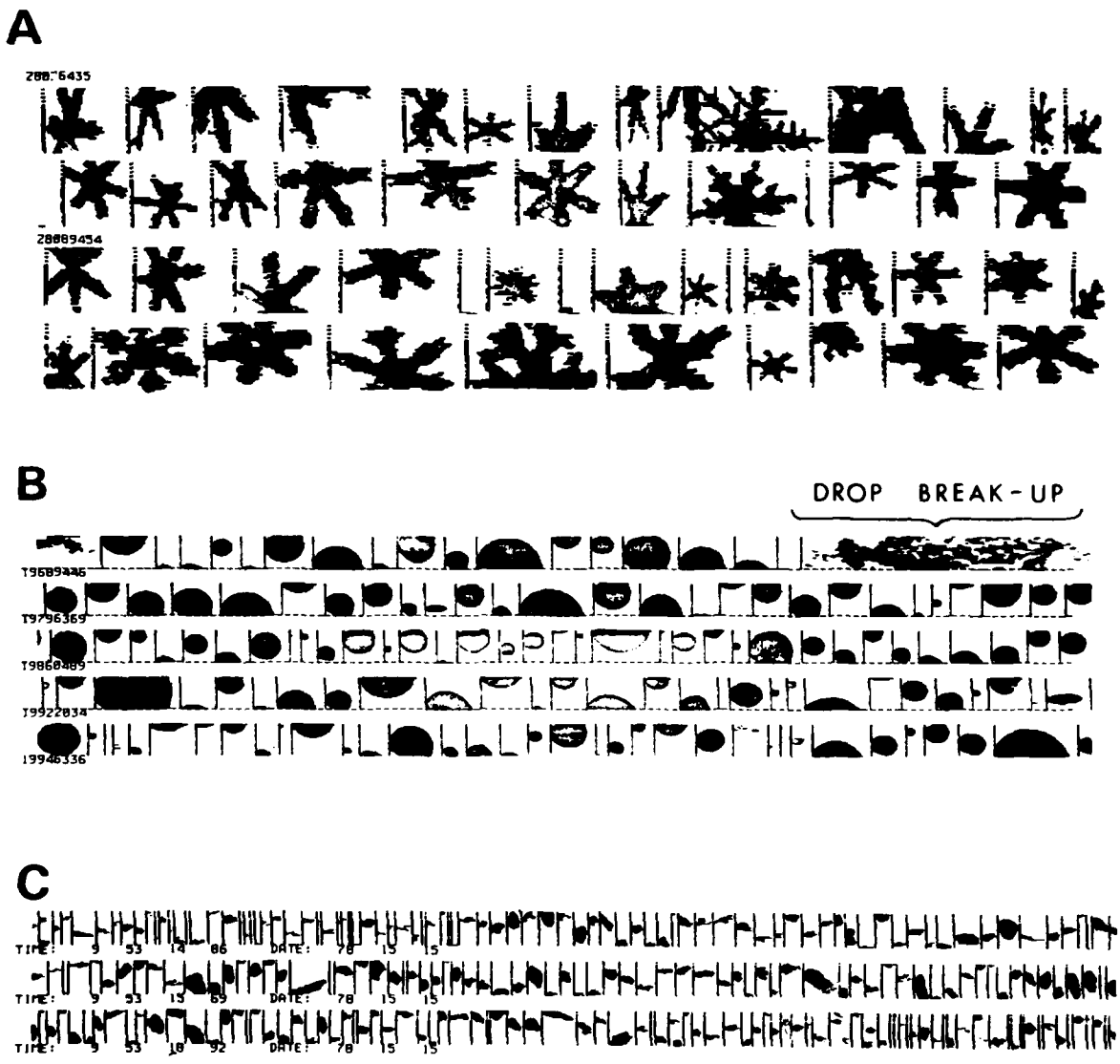

Figure 2.6. Snow (A), Rain (B), and the soil samples (C) from Ground Zero at MISERS BLUFF (see size and mass distributions of Figures 2.3 and 2.4).

The laser output power is measured and provides a signal proportional to the illumination on the particles. Changes in laser output are thus cancelled when the signal is applied as the reference input to the PHA.

A sixteen channel accumulating memory is provided with 20 million population capacity per channel. Each sized particle is stored in one-of-fifteen channels as it is encountered and the sixteenth channel is used for accumulating oversize particles. At the end of each sampling interval, the final values stored are printed out along with the time-of-day and total elapsed seconds for this sample. A separate memory is provided for printing such that the main accumulator memory can be reset immediately and begin sampling for the next interval without interruption during printing.

For the MISERS BLUFF II-2 experiment in which the instrument was used the PMS 206 was fitted with air sampling ductwork to provide an isokinetic air sampling train up to the inlet of the LAS-X (Fig. 2.7). The volume through the air flow duct was approximately 60 ℓ sec^{-1} of which the LAS-X sampled 5 cm^3 sec^{-1}. The LAS-X was set up to run continuously to print out a size distribution every 10 seconds. An auxiliary output was also provided to allow it to input data to the DAS-2D-32. This data was time shared with the 200X through a manual switch multiplexer.

2.2.2 Supporting Measurements and Systems

PMS measured indicated airspeed and the necessary state parameters to compute true airspeed. The sensor is a differential pressure transducer. A measurement of static pressure was used to determine barometric altitude. Free air temperature was measured with a Rosemount platinum resistance temperature sensor, characterized by 0.5 degree accuracy. A stable clock, having better than one part per million stability, was used to provide elapsed time or time-of-day.

The Data Acquisition System was a DAS-2D-32 which has the storage capacity for four separate probes (including 2D) and auxiliary analog and digital inputs. The basic function of the DAS

Figure 2.7: Photograph of external air sampling ductwork used for the LAS-X on MISERS BLUFF II-2.

was to buffer a tape recorder, provide storage, and display data in real time. A block diagram of the data acquisition is presented in Fig. 2.8.

An important aspect of this DAS is the high data framing rate. In MISERS BLUFF II-2 we were able to use 10 frames/second to give 5 to 7 meters resolution in the direction of flight on many parameters.

A standard Pertec Model T-7640-9 Tape Transport with Model F-649-40 Formatter (Table 2.1) recorded the data from the DAS-2D-32. This is 9-track phase encoded equipment for operation at a density of 1600 bytes per inch on standard 7 inch reels (600 feet of tape per reel). Read-after-write units are employed to allow error checking during recording.

PMS also provided a Sony DXC-1600 color video recording system to aid in the post analysis of data by establishing relative cloud penetration data. The DXC-1600 system included video camera controls, and cassette tape recorder. A pilot voice log was also wired into the video record. The system provided one hour recording time per cassette.

2.3 Calibration of Spectrometer Probes

All PMS spectrometers used on MISERS BLUFF II underwent standard static and dynamic calibrations. The static calibrations were generally performed with glass beads and other spheres of known size and refractive index (primary standards). Dynamic calibrations were also performed using the PMS Calibration Wind Tunnel Facility. A description of the PMS Calibration Wind Tunnel Facility is given in Fig. 2.9.

PMS provided dynamic calibrations of the spectrometer probes, both before shipment to MISERS BLUFF and after their return to PMS. This plan insured the integrity of all data collected and was used as inputs to all analysis.

Essentially these dynamic calibrations are intercomparisons with dedicated PMS instrument standards. These standard spectrometers are constantly maintained and seldom leave PMS facilities. Their express purpose is for intercomparisons and test work.

PMS DATA ACQUISITION BLOCK DIAGRAM

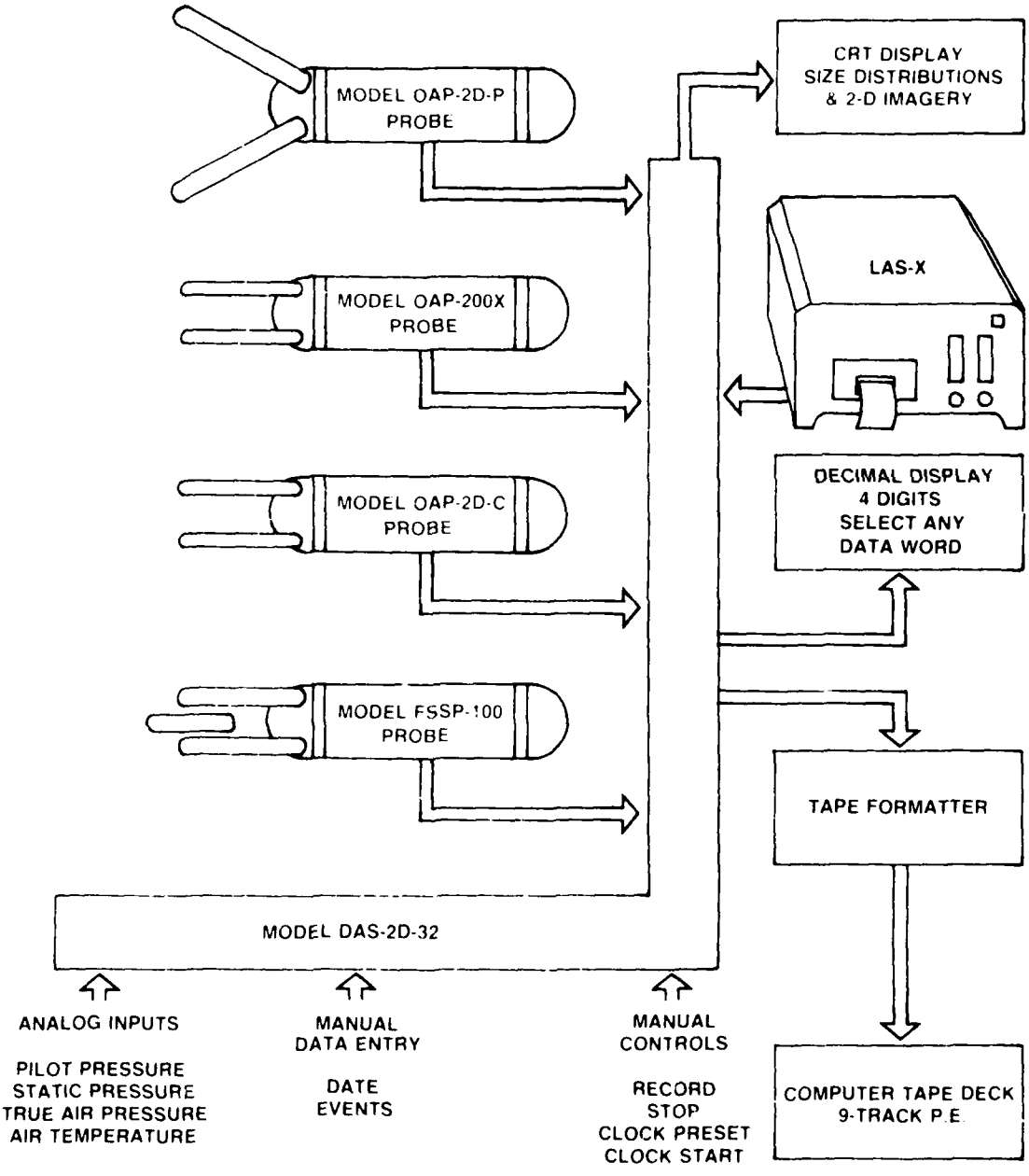

Figure 2.8

PMS CALIBRATION WIND TUNNEL FACILITY

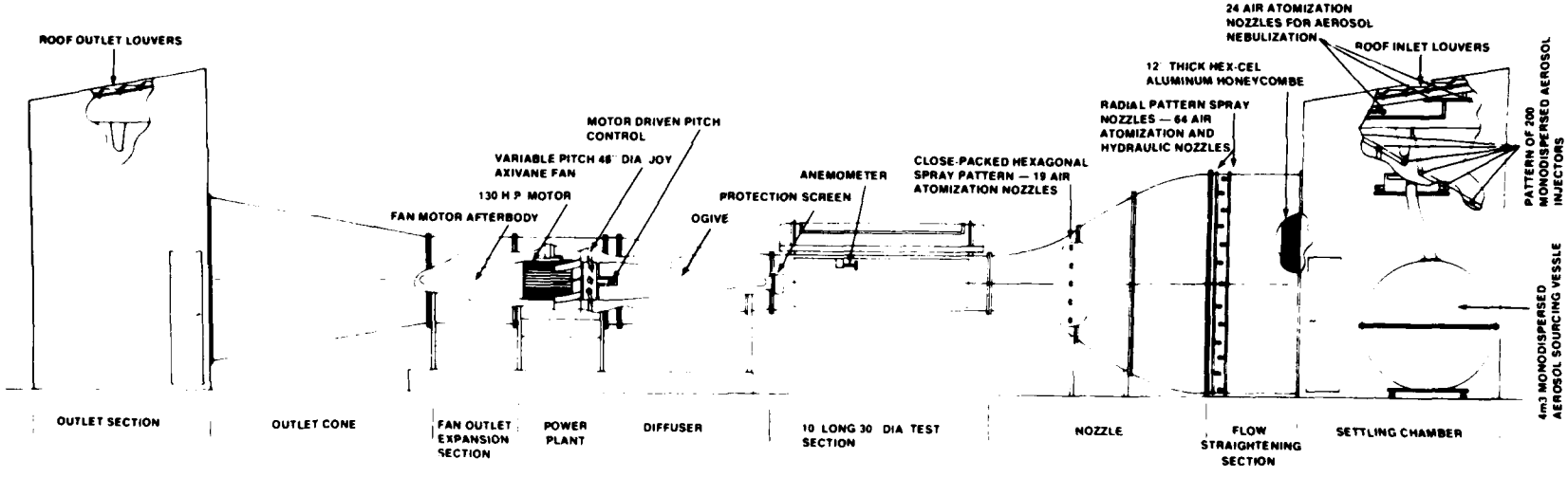

Figure 2.9

2.4 Aircraft Operations Planning

2.4.1 Safety Aspects of the PMS Aircraft Operations

During early fallout measurements and intensive dust cloud sampling considerable attention was directed to overall safety even though substantial aircraft damage was not expected. Essentially five hazards were identified:

Particulate ingestion into engine with possible power loss.

Particle impact erosion and damage.

Extreme turbulence in cloud stem.

Proximity of other aircraft and dropsondes released by other aircraft.

Laser hazards.

The standard Cessna 206 engine inlet air filter was expected to become saturated soon after cloud sampling began. An automatic alternate air inlet is incorporated in the Cessna 206 which directs unfiltered alternate air to the engine whenever the air filter becomes clogged. The alternate air travels a reverse-flow path which should remove all particles larger than about 50 μm. Those ingested particles could cause considerable engine wear during the mission. Planning called for the engine to be partially disassembled and borescoped after Event 1 to determine the extent of damage. A decision could then be made whether to retain the aircraft at the test site between events 1 and 2 to preclude accelerated wear due to sand particles trapped in the cylinders. However, an oil soaked prefilter was installed in the air inlet ductwork prior to MISERS BLUFF II-1. This coupled with the fact that the alternate air source was not opened during dust penetrations precluded any necessity for detailed examination.* However, after MISERS BLUFF II-2 engine rebuilding was required.

* The alternate air door was configured with a microswitch and a pilot panel warning light to give the pilot a positive indication of door opening.

The large low-level fallout particles can cause considerable impact damage, particularly to the aircraft paint, leading surfaces, cowling and windshield. While we expected that repair might be substantial, the damage was not expected to be severe enough to disable the engine or aircraft structure. As a very simple precaution, PMS arranged to have a crude emergency landing strip graded approximately one mile west of Ground Zero.

The extreme turbulence associated with the cloud stem must be avoided until updraft velocities diminish. Comparisons of updraft velocities measured in prior events and physical observation of the rising clouds were used to determine cloud updraft velocity and turbulence levels. Essentially all penetrations revealed only light turbulence at times beyond T+3 minutes.

Traffic separation did not present any significant problems. However, the dropsondes released by the Kaman Sciences Aircraft constrained the early sampling by the PMS 206 as well as any other sampling aircraft. With regard to the potential hazards of multi-aircraft operations at MISERS BLUFF cloud sampling efforts had to be coordinated with all other aircraft as pointed out above. To this end a positive radar control (temporary restricted) area was set up and separation from all experiment (as well as visitors) aircraft provided by the 3rd Combat Communications Group (3CMBTCG), Tinker AFB, Oklahoma.

The high energy lasers used for LIDAR observations and transmissometry at MISERS BLUFF presented a potential hazard to viewers from aircraft. To safeguard any possible eye contact safety goggles were provided and worn by all PMS personnel aboard the PMS 206 aircraft.

2.4.2 Flight Profiles

Considerable attention was given the problem of attempting an early entry to acquire large particles that fall out the first few minutes following detonation. We decided to use experiential judgment on when to penetrate and were restricted by dropsonde activity in MISERS BLUFF II-2.The early entry requirement dictated an arrival over Ground Zero at as low an altitude as safety could

permit. We decided to make penetrations at fixed altitudes and headings using the out-of-cloud time to turn and climb giving 500 to 1000 foot intervals between passes. The turns were designed as modified procedure turns to provide course reversal in the least amount of time. We also desired to penetrate the cloud near its center during each pass so that measurements would be made along the maximum diameter of the dust cloud parallel to the mean wind direction.

3.0 EXPERIMENT DESCRIPTIONS AND RESULTS

The results of the air sampling of dust particles during MISERS BLUFF II presented here should be regarded as an overview. The detailed analysis of this data requires a great deal more study and is beyond the scope of this report. However, a detailed data set was obtained, processed, and submitted under separate cover. Much of the in-depth analysis of these processed data records will be reported on by Science Applications, Inc. (DNA #001-78-C-0217). In addition, preliminary data submittals were provided DNA a few weeks after each event as Quick Look Reports (actually these Quick Look Reports included detailed data processing). This current report should be looked upon as an interpretive aid when examining all MISERS BLUFF II data processed by PMS.

Most importantly,this section summarizes those important particle parameters which characterize MISERS BLUFF II-1 and MISERS BLUFF II-2. Because these experiments were designed as a paired set both experiments will be described and compared as a set. Because of the more extensive instrument grouping for MISERS BLUFF II-2 as compared to MISERS BLUFF II-1, the nearly 100% operation of equipment, and the more massive cloud volume and thus data set gathered, more attention is given MISERS BLUFF II-2. We will begin with a general description of flight operations of both experiments, followed by our treatment of the experimental results with an examination of the dust cloud mass and optical properties.

3.1 Base Operations and Flight Preparations

The Cessna 206 aircraft fielded by PMS for the MISERS BLUFF II exercises was based at Lake Havasu City, Arizona. Fueling and maintenance facilities proved adequate as evidenced by a quick refueling turnaround required during an extended hold on MISERS BLUFF II-1. Hangar space was available but proved unnecessary for the aircraft as only external power was required for routine operational checks on the instrumentation. No direct communications with the Field Command Defense Nuclear

Agency were available at the airport; however, preplanning obviated the need for such.

Prior to the ferry flight to Lake Havasu City, all on-board instrumentation was thoroughly checked for proper operation. In addition to the calibration work (see Section 2.3) this included ground checks and flights into natural weather conditions such that all spectrometer probes, data systems, and real-time displays would be exercised. Tape processing reinforced the expected and observed operations.

A dry run exercise was carried out two days before MISERS BLUFF II-1 primarily to guarantee that communications and traffic separation were properly staged. Between the dry run and the shot on MISERS BLUFF II-1, the aircraft was further prepared and safeguarded with a plastic cover over the windscreen, an oil-impregnated air filter in the induction system, and all air inlets taped closed to exclude as much dust as possible from both the engine, the aircraft, and the occupants. Some of this procedure was modified for MISERS BLUFF II-2.

As the oil impregnated sponge filter supplementing the aircraft air induction filter became clogged with dust cloud debris, the alternate air source door would open (a signal light was installed on the pilot's panel) but this was only observed when full power was applied on climbs outside the cloud on MISERS BLUFF II-1. On MISERS BLUFF II-2, with its greater dust cloud size and mass loading, the alternate air source door was opened much earlier and was intermittant at all power settings above 24" manifold pressure on most passes.

A thorough ground check of all systems was made just prior to takeoff on each flight and stored on tape. In MISERS BLUFF II-1, the equipment was left on; however, in MISERS BLUFF II-2, the equipment was powered down until T-10 minutes to conserve aircraft power and to preclude heat buildup in the instrumentation and cabin.

3.2 MISERS BLUFF II Flight Operations: A Narrative Summary

In each phase of the MISERS BLUFF II exercise, the PMS sampling aircraft proceeded to the T-20 minutes rendezvous point over the Sansea pumping station. Initial holding altitude was above 5K MSL to provide a cooler environment for equipment and personnel. A gradual descent was made to arrive at the initial penetration altitude at T-0 minutes.

The following paragraphs of detailed flight operations apply to MISERS BLUFF II-1 conducted on 28 June 1978.

The first sampling pass after T=0 minutes (13:05 MST) was upwind of the stem and west of the main dust cloud which had drifted over the bluff precluding safe flight under the main cloud. The second pass was in the same region ostensibly to detect the fallout of large particles as was the first.

The third through fifth passes were made in the stem of the cloud and the visibility was very poor. The 2D precipitation probe was disconnected at the end of pass #3 due to its constant update condition and lack of data in its size range.

Pass #6 was in the base of the cloud following an altitude increase and showed an increase in 2D-C particle concentration. All subsequent penetrations were at selected higher altitudes in the dust cloud. The 2D precipitation probe was activated briefly on pass #8 with continued negative results.

Heat buildup in the cabin due to closure of aircraft vents (taped) was alleviated by opening the window when maneuvering out-of-cloud. Following pass #12 at about 13:21, a smoke odor was noticed in the aircraft cabin,its source being other than combustion. Electrical problems were suspected about 5 minutes later when false 2D records appeared. Subsequent

aircraft charging problems were noticed along with more smoke and probes were cycled off when out-of-cloud to conserve battery power. At 13:50 data quality was determined to be rather poor and by 13:58 return to Lake Havasu City airport was warranted.
Ground checks revealed a thermally sensitive preamp in the 2D-P instrument which was easily diagnosed and corrected. No damage to the aircraft was visible and the electrical problem was quickly diagnosed as a poor contact on the alternator ground wire.

For MISERS BLUFF II-2 there were some modifications to the aircraft. As stated previously, a fifth instrument, an LAS-X was installed in the cabin with the necessary ducting and plumbing to sample externally. Data from this probe was time shared with data from the 200X as the DAS-2D-32 could handle only four probes. The windshield was not covered with plastic as in MISERS BLUFF II-1, as no large or abrasive debris had been encountered then, and the aircraft induction system and cabin vents were fitted with pieces of the oil-impregnated sponge filter material. This permitted the usage of cabin air vents during sampling for ventilation. In order to conserve aircraft power, the equipment was checked on the ground before take-off then powered down until T-10 minutes. A higher (and cooler) altitude was also used for holding on MISERS BLUFF II-2.

The following paragraphs of detailed flight operations apply to MISERS BLUFF II-2 conducted on 30 August 1978:

The first data pass was made approximately 4.5 minutes after T=0 (11:00 MST) and was downwind of the dust cloud stem and under the most massive part of the cloud. The pass was flown at 2.5 K MSL (1.7K AGL) in order to be in the densest area of dustfall. Much larger, friable

debris were collected on the aircraft windshield on this pass than on the first pass of MISERS BLUFF II-1.

Because of the apparent absence of *hard* particles, the next three passes were made into the stem of the dust cloud at successively higher altitudes. On pass #4, the alternate air source light was observed for the first time--an indication of insufficient induction airflow through the filter.

Pass #5 was the first pass truly within the dust cloud itself just above the base of the cloud. It was quite dark within the cloud with the ground just discernible but horizontal visibility essentially zero. On pass #6 the light loss in the cloud seemed the greatest and persisted for about 45 seconds. Visual contact with the ground was lost for part of that time and there was no horizontal or overhead visibility.

On pass #7, in-cloud time was longer (at least 1 minute) but overhead light extinction was less than on the previous two passes. Progressively more overhead light was observed on subsequent passes as the aircraft was climbing at a rate greater than that of the ascending cloud. On at least part of the cloud penetration track, visual ground contact was lost due to the increased cloud mass between the aircraft and ground.

Passes #8-12 proceeded to the top of the dust cloud in increasing altitude steps. Visual observations were much as expected with greater overhead light and increased horizontal visibility along with obscuration of ground contact due to the cloud mass being below the penetration level. Pass #12 at 13K was just at the cloud top which appeared to be rather sharp and uniformly flat.

Passes #13-18 were at step-down altitudes from 13K to 3K and were essentially repeats of the step-up altitude passes with overall visibility improvements due to cloud thinning, a result of particle dilution. Most of the passes were made in essentially IFR conditions but an obvious improvement in visibility was noted from previous passes. A desired result of these step-down passes (#13-18) was to detect the fallout of large particles.

At the end of pass #18, approximately one hour after pass #1, the aircraft was located some 20 to 30 nm North of Ground Zero and still collecting particle sizes in all five probe ranges. This gives one an indication of the magnitude of the dust cloud, its lofting ability, carrying capacity, and overall relationship to the dust cloud of MISERS BLUFF II-1.

Passes #19-22 were made on various headings at increasing altitudes from 3K to 8K feet. These four passes were essentially altitude repeats of passes #15-18 and following their completion, the aircraft returned to base.

After landing, all spectrometer probes were ground checked for proper operation before shutdown. The aircraft was thoroughly checked, cleaned, and inspected for any damage. The greater mass load of the MISERS BLUFF II-2 cloud warranted an aircraft compression check which was within specifications; however, it rapidly deteriorated with a few more hours of flying time and as previously indicated an engine change was warranted.

All instruments were again recalibrated after return to PMS. Of worthy note was the contamination of the FSSP optical system and reduced sensitivity which was obvious in data analysis.

The sampling experiments carried out with the PMS 206 aircraft were considered quite successful even though several problems were encountered. Essentially two problems occurred on MISERS BLUFF II-1 that were prevented from occurring on MISERS BLUFF II-2. On MISERS BLUFF II-1 the 2D-P probe developed an oscillation in a second stage preamp due to the high temperatures (>120°F) at the Lake Havasu City airport.* This caused the instrument to constantly *update* with noise and was turned off during the experiment when the data obtained were determined to be of negligible value. The second problem had to do with an eventual electrical failure on the aircraft alternator near the end of the sampling mission. The problem was isolated to ground wiring,which while not easily related to the experiment, the coincidence seems to point to possible thermal or dust environment causation. The sampling mission was completed under battery power. MISERS BLUFF II-2 saw essentially 100% operation of all instrumentation aboard the aircraft. The only factor of note was a gradual soiling of the FSSP collecting optics which reduced it's sensitivity during the course of the measurements.

3.3 Experimental Results

The sampling missions for MISERS BLUFF II-1 and MISERS BLUFF II-2 were approximately one hour each in duration. In both cases the in-cloud time was approximately one-third to one-half the total time amounting to 1000 seconds on MISERS BLUFF II-1 and 2000 seconds on MISERS BLUFF II-2. Fig. 3.1 and 3.2 are photographs of the dust clouds generated a few minutes after detonation. The MISERS BLUFF II-1 photograph in

* Actually the problem developed during a necessary refueling stop necessitated after the experiment was placed in *hold* condition too long for it to remain airborne and perform the sampling mission.

MISERS BLUFF II-1 DUST CLOUD

Figure 3.1: Photograph of dust cloud taken from SRI International's Main Transmitter Site, 1.2 km southeast of ground zero. (Photograph compliments of Stanford Research Institute).

MISERS BLUFF II-2 DUST CLOUD

Figure 3.2. Photograph of the dust cloud taken from the PMS 206 aircraft approximately 2 nm Southeast of Ground Zero at an altitude of 300 m AGL 4 min. after detonation.

Fig. 3.1 was taken by Stanford Research Institute (SRI) International personnel from 1.2 km southeast of ground zero. The PMS 206 aircraft is in the lower cloud at the time the photograph was taken in Fig. 3.1. The MISERS BLUFF II-2 photograph in Fig. 3.2 was taken from the PMS-206 aircraft approximately two miles out and 60 seconds before initial entry. The photograph is from a stage in cloud development wherein the large particle fallout (>2 mm) is nearly complete (T=+4 minutes). It also reveals the developing large vortex ring and a higher cloud puff which was forced out of the central core.

MISERS BLUFF II-1 and MISERS BLUFF II-2 dust clouds were sampled in 21 and 22 cloud pass penetrations respectively. The dust cloud parametric summaries are given in Tables 3.1 and 3.2. The orientation and ground tracks for the step-up passes are shown in Figs. 3.3 and 3.4 for both experiments. The summaries in Tables 3.1 and 3.2 include results of data analysis and processing which will be discussed in more detail later. First we will briefly cover more general features.

As previously mentioned the initial penetrations were from the southeast at headings of 320 to 330°. First passes were at T+2.5 minutes and T+4.5 minutes for MISERS BLUFF II-1 and MISERS BLUFF II-2. Both initial passes were aimed at measuring fallout underneath the overhang beside the stem.

In order to characterize the clouds, step-up profiles were used.* In MISERS BLUFF II-1 the cloud was topped in 18 passes while 12 were required in MISERS BLUFF II-2. By the time the top was reached the cloud had risen to 2.8 and 3.7 km AGL for MISERS BLUFF II-1 and MISERS BLUFF II-2 requiring 22 and 32 minutes respectively. After reaching cloud top sampling continued

* The step-up passes provided one complete set of cloud data. During step-down most other experiments had ceased and ground tracking is incomplete.

Table 3.1

MISERS BLUFF II-1 28 JUNE 1978

DETONATION @ 13:05 MST

PASS NO	ALTITUDE	HEADING	TRUE AIRSPEED	TIME ENTER	TIME EXIT	PASS TRANSIT TIME	PASS WIDTH	MAXIMUM SIZE	MASS LOADING	CROSS SECTIONAL MASS LOADING	OPTICAL DEPTH	EXTINCTION COEFFICIENT		VISIBILITY	
								mm				Km^{-1}		Km	
	km (AGL)	Degrees	$m\ sec^{-1}$	(MST)	(MST)	SEC	m	2D-C	gm^{-3}	$Kg\ m^{-1}$		Avg	Peak	Avg	Min
1	.34	330	57.65	13:07:23	13:07:39	16	922	.375	7.89×10^{-2}	5.26×10^{1}	.501	5.69	21.7	.70	.18
2	.30	060	60.23	:08:15	:08:36	21	1264	.125	5.45×10^{-2}	6.83×10^{1}	2.42	2.32	12.1	1.72	.33
3	.30	260	60.23	:08:52	:09:05	13	783	.300	6.72×10^{-1}	3.15×10^{2}	30.8	4.75	98	.08	.041
4	.36	040	60.23	:09:37	:09:51	14	843	1.250	3.43×10^{-1}	1.91×10^{2}	21	30	48	.13	.083
5	.41	200	60.23	:10:36	:11:09	33	1987	.625	1.27×10^{-1}	3.91×10^{2}	10.1	6.17	33.9	.65	.12
6	.55	360	60.74	:11.34	:11:47	13	789	.500	2.32×10^{-1}	1.14×10^{2}	6.94	10.6	24.2	.38	.16
7	.67	165	61.26	:13:33	:14:08	35	2144	.500	1.16×10^{-1}	4.19×10^{2}	11.5	6.47	21.8	.62	.18
8	.79	340	63.83	:15:16	:15:38	22	1404	.275	8.81×10^{-2}	1.37×10^{2}	6.30	5.43	15.7	.73	.25
9	.79	140	61.77	:16:03	:16:31	28	1729	.375	7.43×10^{-2}	1.75×10^{2}	7.37	5.15	18.1	.77	.22
10	1.04	300	64.86	:17:58	:18:25	27	1751	.250	9.13×10^{-3}	2.20×10^{1}	1.23	.85	2.66	4.68	1.50
11	1.22	195	66.92	DATA INSUFFICIENT TO ANALYZE											
12	1.28	050	57.65	:20:47	:21:55	68	3920	.450	4.28×10^{-2}	5.18×10^{2}	7.66	2.36	6.05	1.69	.66
13	1.58	220	61.26	:23:37	:24:50	73	4472	.700	4.14×10^{-2}	6.53×10^{2}	7.55	2.04	4.24	1.95	.94
14	1.89	010	71.04	:28:33	:29:41	68	4830	.350	4.14×10^{-2}	6.49×10^{2}	8.56	2.14	4.24	1.86	.94
15	1.89	225	65.38	:30:41	:32:04	83	5426	.725	DATA INSUFFICIENT TO ANALYZE						
16	1.89	000	59.20	:33:05	:34:28	82	4854	.375	2.94×10^{-2}	5.38×10^{2}	6.85	1.71	4.24	2.33	.94
17	1.89	195	65.38	:35:50	:37:44	114	7453	.350	1.90×10^{-2}	8.26×10^{2}	8.39	1.36	3.63	2.93	1.1
18	2.80	330	74.13	DATA INSUFFICIENT TO ANALYZE											
19	1.89	210	65.38	:50:07	:52:30	83									
20	1.89	320	65.38	:53:22	:54:43	81	DATA OF QUESTIONABLE VALIDITY (ALTERNATOR FAILURE)								
21	1.89	100	62.29	:55:14	:57:16	122									

Table 3.2

MISERS BLUFF II-2 30 AUGUST 1978

DETONATION @ 11:00 MST

PASS NO	ALTITUDE	HEADING	TRUE AIRSPEED	TIME ENTER	TIME EXIT	PASS TRANSIT TIME	PASS WIDTH	MAXIMUM SIZE (mm)		MASS LOADING	CROSS SECTIONAL MASS LOADING	OPTICAL DEPTH	EXTINCTION COEFFICIENT (Km^{-1})		VISIBILITY (Km)	
	km (AGL)	Degrees	m sec^{-1}	(MST)	(MST)	SEC	m	2D-P	2D-C	gm^{-3}	Kg m^{-1}		Avg	Peak	Avg	Min
1	.52	320	49.94	11:04:34	11:04:51	17	879	1.3	.250	.25	1.566×10^{2}	.404	.552	1.56	7.21	2.55
2	.67	120	56.12	:06:07	:06:28	21	1223	2.0	.750	.35	4.205×10^{2}	7.52	7.38	24	.54	.16
3	.79	320	50.46	:07:35	:08:16	41	2099	1.6	2.250	.09	3.538×10^{2}	5.08	2.91	14.4	1.37	.28
4	1.13	180	51.49	:09:45	:10:23	38	1925	1.2	1.425	.23	6.989×10^{2}	6.78	8.45	26.4	.47	.15
5	1.49	020	52.01	:11:43	:12:56	73	3724	1.0	.800	.12	1.20×10^{3}	13.1	5.84	31.2	.68	.13
6	1.89	200	53.55	:14:37	:15:30	53	2827	1.3	.825	.41	2.584×10^{3}	30.5	15.98	42	.25	.09
7	2.31	050	54.58	:17:22	:18:17	55	3001	1.0	.950	.17	1.215×10^{3}	25.7	10.26	26.4	.39	.15
8	2.50	210	55.09	:19:48	:20:59	71	3911	.8	.575	.23	2.53×10^{3}	25.8	12.36	33.6	.32	.12
9	2.74	040	61.79	:23:16	:24:42	85	5264	1.0	.800	.099	2.15×10^{3}	21.4	4.88	14.4	.82	.28
10	3.02	190	62.82	:25:39	:27:13	94	5867	.9	.900	.189	5.10×10^{3}	45.2	8.48	34.8	.47	.11
11	3.26	060	57.15	:29:39	:31:29	110	6286	.6	.350	.058	1.68×10^{3}	11.5	4.4	14.4	.90	.28
12	3.72	240	64.88	:34:31	:36:39	128	8304	.3	.075	.00003	<15	<.83	<0.1	<0.1	>40	>40
13	3.26	070	63.33	:38:33	:41:20	107	6776	.4	.575	.029	1.12×10^{3}	9.28	3.3	12.4	1.21	.32
14	2.80	240	61.79	:41:20	:43:06	106	6549	.9	.400	.015	5.71×10^{2}	6.15	2.24	7.2	1.78	.55
15	2.19	050	60.24	:45:41	:47:27	104	6265	.5	.400	.006	1.95×10^{2}	3.78	.72	3.36	5.53	1.18
16	1.59	220	64.36	:51:10	:53:17	127	8173	.7	.600	.009	4.67×10^{2}	9.12	1.33	3.0	2.99	1.32
17	1.13	045	57.15	:55:48	:57:49	121	6915	1.1	.425	.038	1.45×10^{2}	8.64	1.50	5.0	2.65	.80
18	.67	210	56.12	12:00:20	12:02:17	117	6566	.6	.625	.0038	1.28×10^{2}	4.11	.76	3.1	5.24	1.28
19	.67	Turn	50.46	:03:39	:07:06	207	10.445*	.7	.425	.0041	3.45×10^{2}	4.52	.52	3.6	7.65	1.11
20	1.28	210	54.58	:07:19	:09:14	115	6276	.6	.350	.0015	5.19×10^{1}	2.15	.41	.96	9.71	4.15
21	1.74	020	58.70	:09:58	:11:34	96	5635	.5	.450	.006	1.42×10^{2}	1.47	.62	2.4	6.42	1.66
22	2.19	210	60.42	:15:36	:17:22	106	6404	.7	.675	.017	4.23×10^{2}	3.36	1.26	4.1	3.3	.97

* Insufficient data (no analysis)

MISERS BLUFF II-1 PMS-206 GROUND TRACK

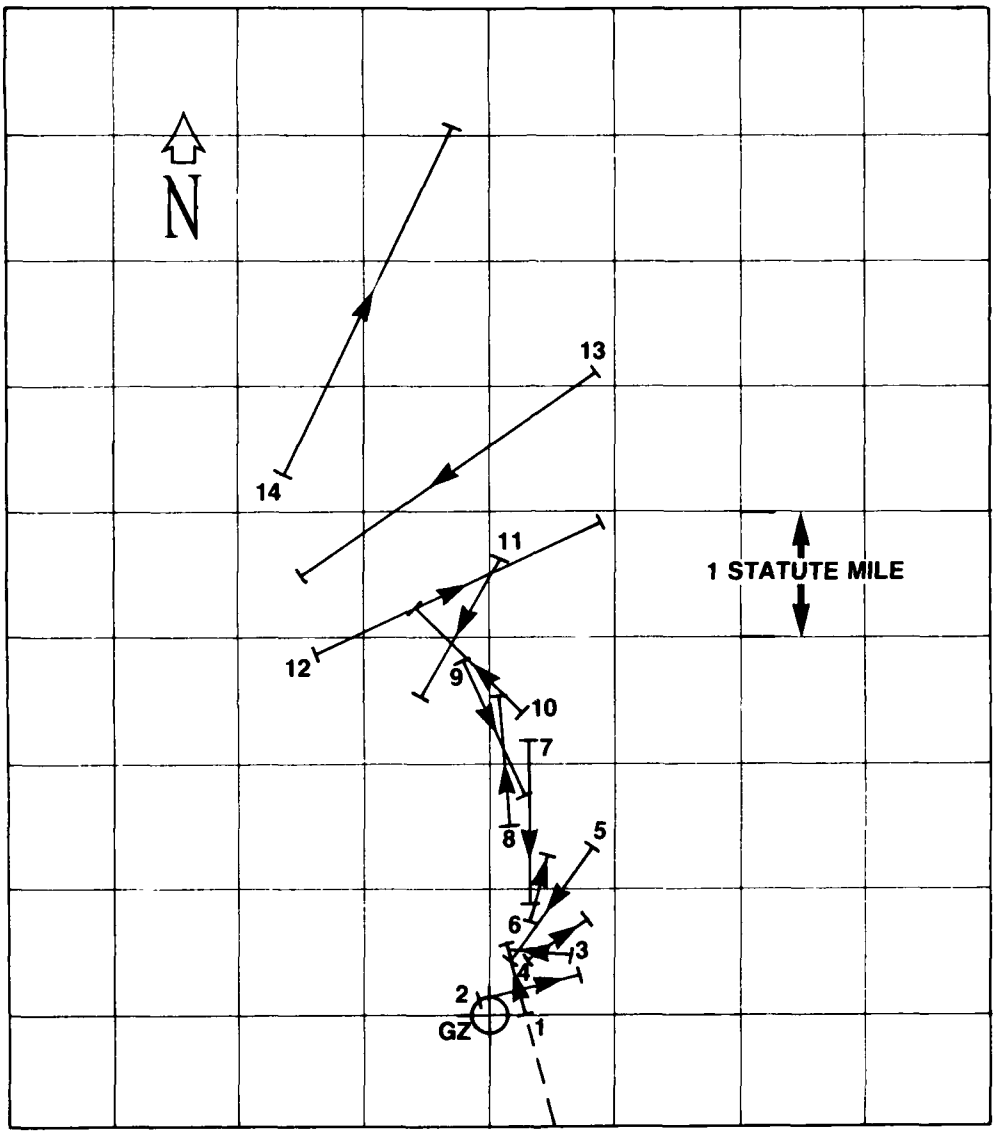

Figure 3.3

MISERS BLUFF II-2 PMS-206 GROUND TRACK

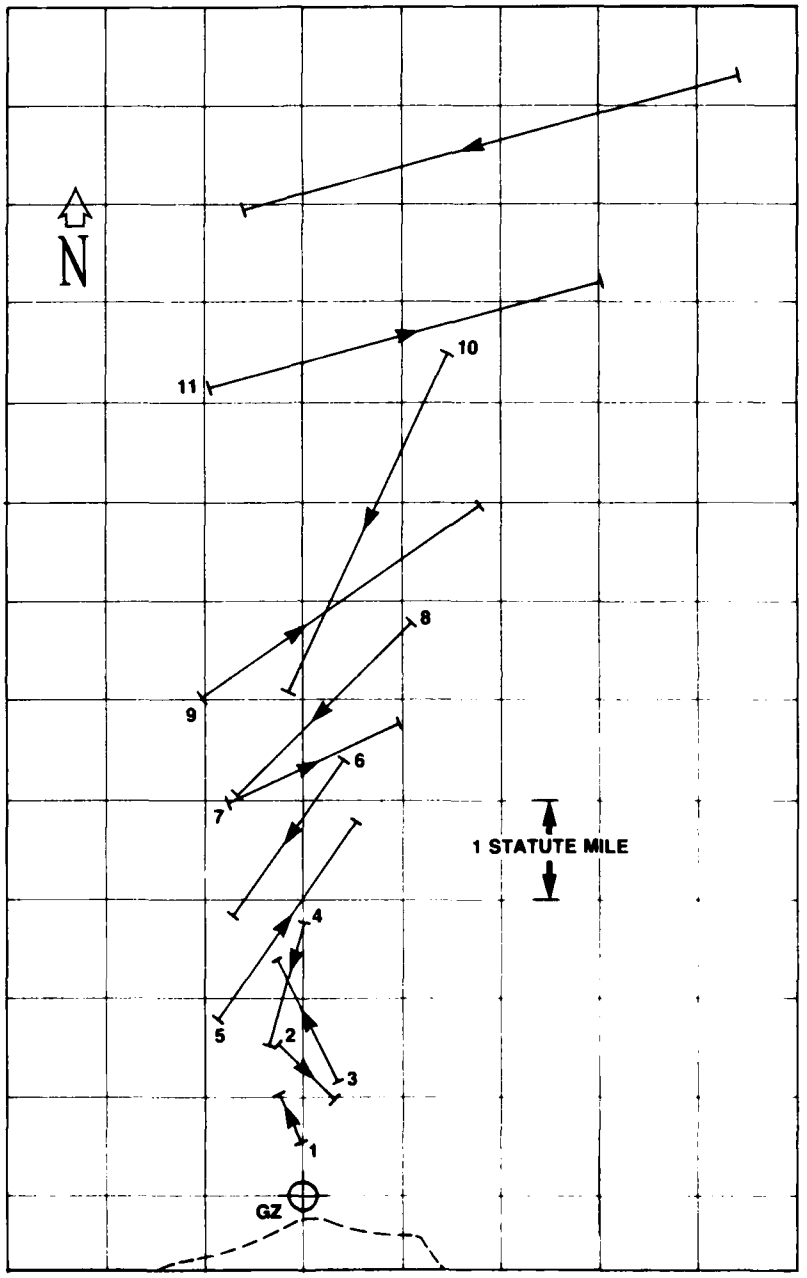

Figure 3.4

in step-down profiles. The step-down passes provide an additional data set; however, their analysis is not necessary to characterize the cloud and must be excluded when determining integrated cloud properties such as total mass lofted. The step-up profiles could essentially be referred to as the cloud characterization passes. The maximum cloud width occurred near the cloud top in both clouds expanding to 4800 meters in MISERS BLUFF II-1 and 8300 meters in MISERS BLUFF II-2. The clouds were penetrated at velocities of approximately 60 m sec^{-1} during both experiments.

An interesting comparison of dimensional data is available from ground photography and the PMS 206 measurements. Fig. 3.5 and 3.6 indicate altitudes of PMS 206 measurements with respect to photographic data while Fig. 3.7 and 3.8 depict cloud width measurement comparisons. Fig. 3.7 and 3.8 show that the cloud width measurements by the PMS 206 and photographic means for MISERS BLUFF II are in reasonable agreement. However, Fig. 3.5 shows considerably higher cloud tops by photography than revealed by the PMS 206. This may be due to differences in measurement times but if true the cloud top must have had an overshoot at earlier times. Fig. 3.6 indicates several initial passes below the stem top followed by cloud penetrations up through pass #12 which as previously indicated topped the cloud. Assuming that the top of the cloud did not sink between T+30 minutes and T+35 minutes it would again appear that the photographic estimates are high (about 300 to 400 meters) in estimating cloud top. We should also point out that stem top is typically higher than the cloud base in early cloud development.

The cloud width measured by the PMS 206 would be expected to be systematically somewhat less than that revealed by photography. This is partially due to the fact that the aircraft was generally not penetrating at the level of maximum width. However, top differences at high altitude are larger than would be expected. The aircraft penetrations were aligned with the wind and possibly the photographic results reveal the shear in the vertical cloud structure. In any case we cannot account for differences as large as indicated. Pressure altitude should be accurate to ±100 feet

MISERS BLUFF II-1 PMS 206 PASS ALTITUDES COMPARED TO PHOTOGRAPHIC CLOUD RISE DATA

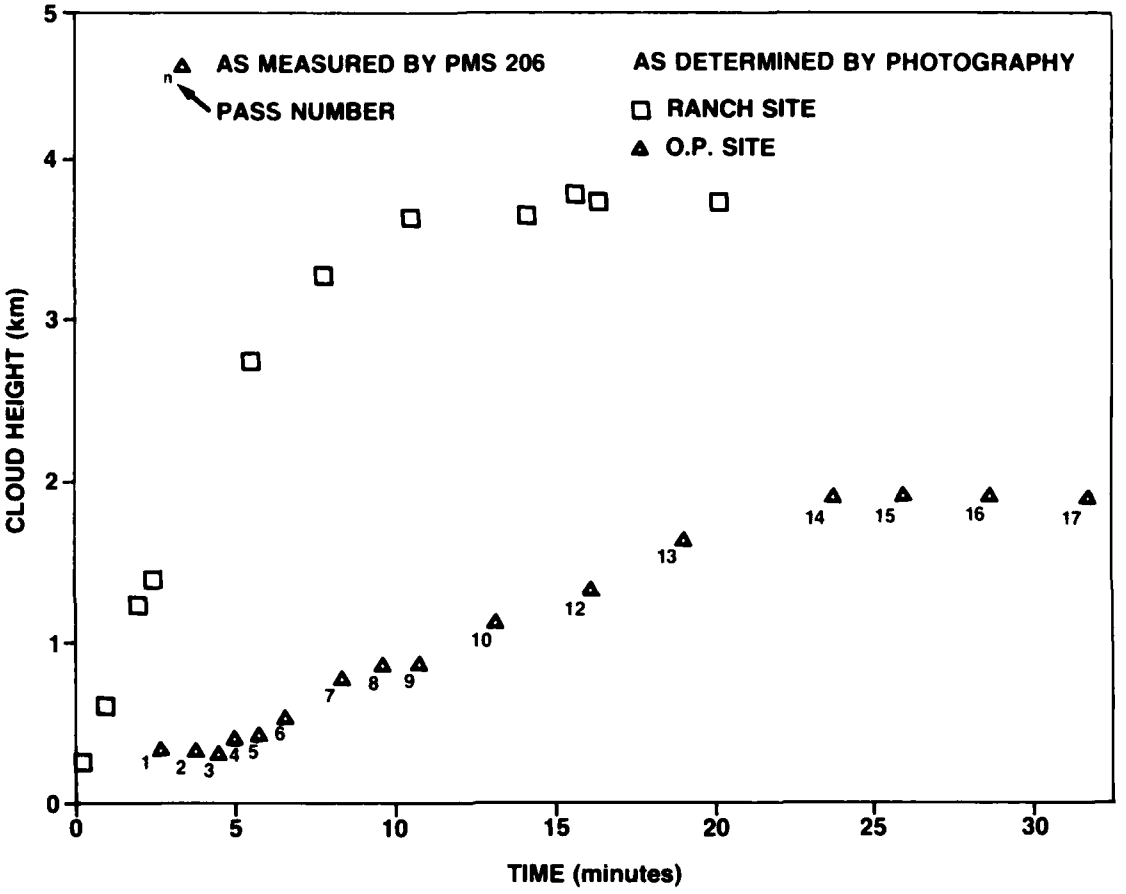

Figure 3.5: Analysis of photographic data furnished by Technology International Corporation. Pass #17 was just below top and #18 topped cloud at 2.8 km.

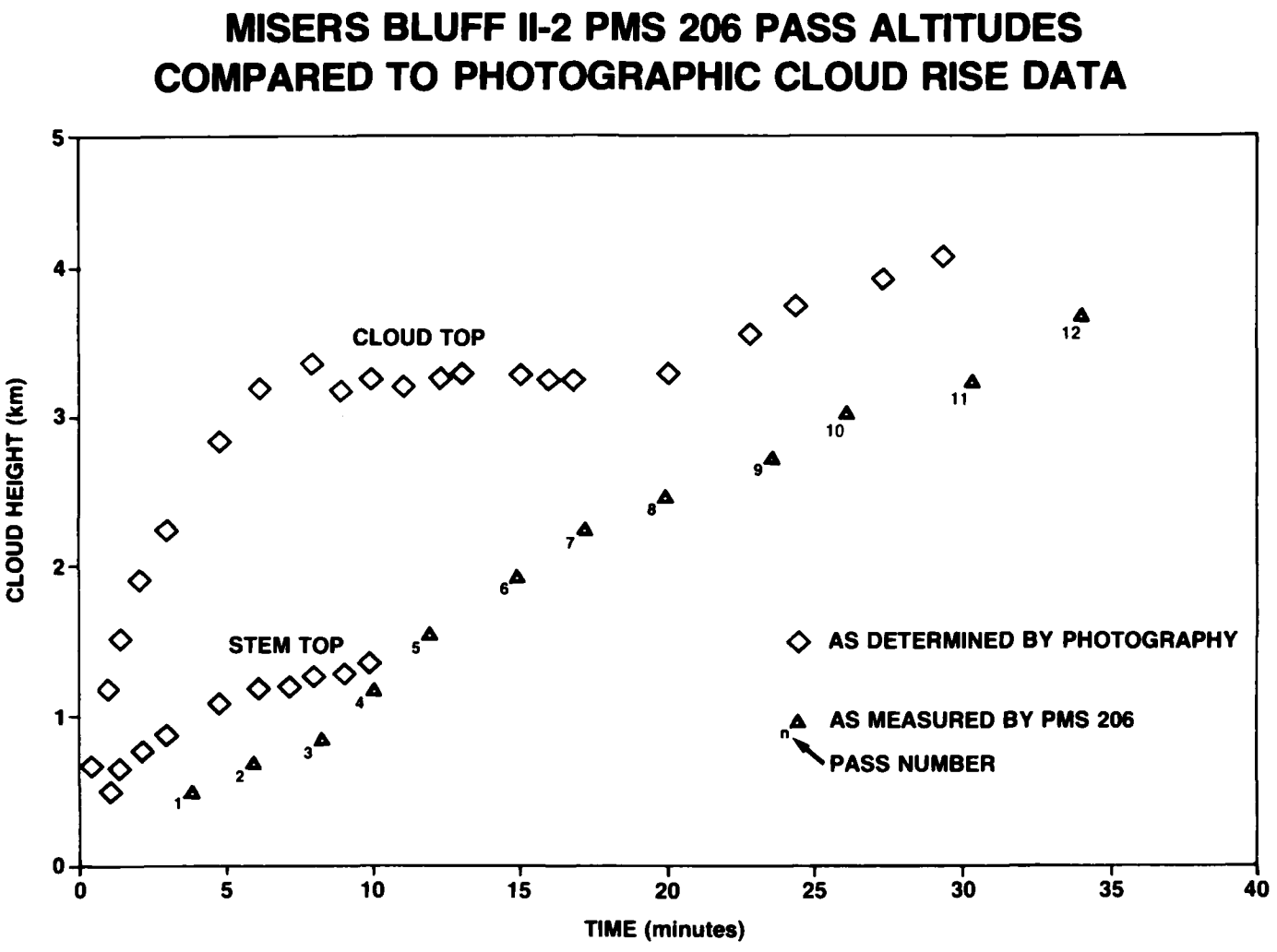

Figure 3.6: Note that it is possible for the stem to be higher than the cloud base. (Analysis of photographic data furnished by Technology International Corporation).

MISERS BLUFF II-1 CLOUD WIDTH MEASUREMENTS

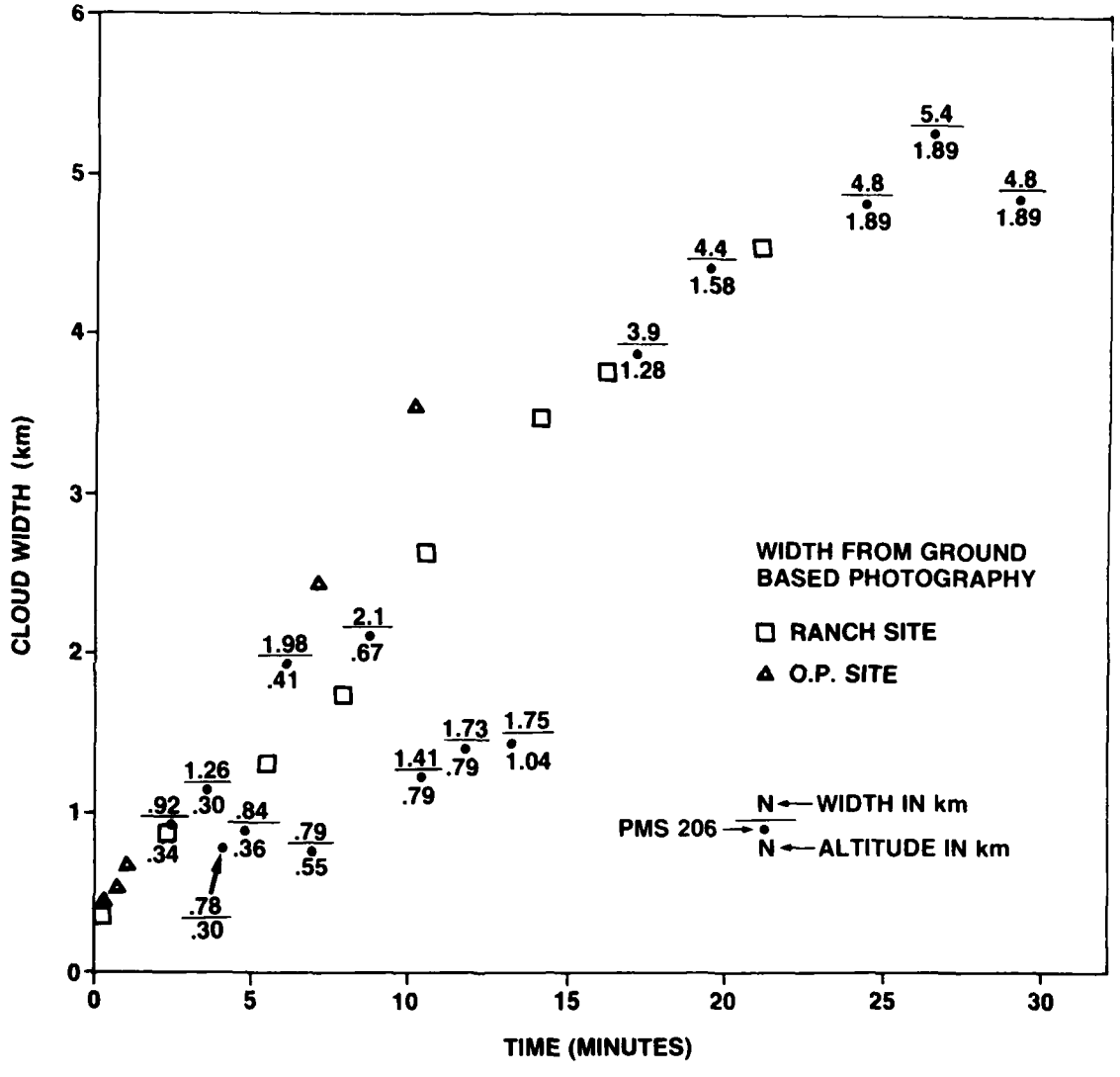

Figure 3.7: The cloud width measurements as deduced by analysis of ground based photographs and from the PMS 206 measurements are seen to be in reasonable agreement at times beyond 10 minutes. One may interpret this to imply that the PMS 206 passes were made through the most extensive cloud regions (analysis of photographic data furnished by Technology International Corporation).

MISERS BLUFF II-2 CLOUD WIDTH MEASUREMENTS

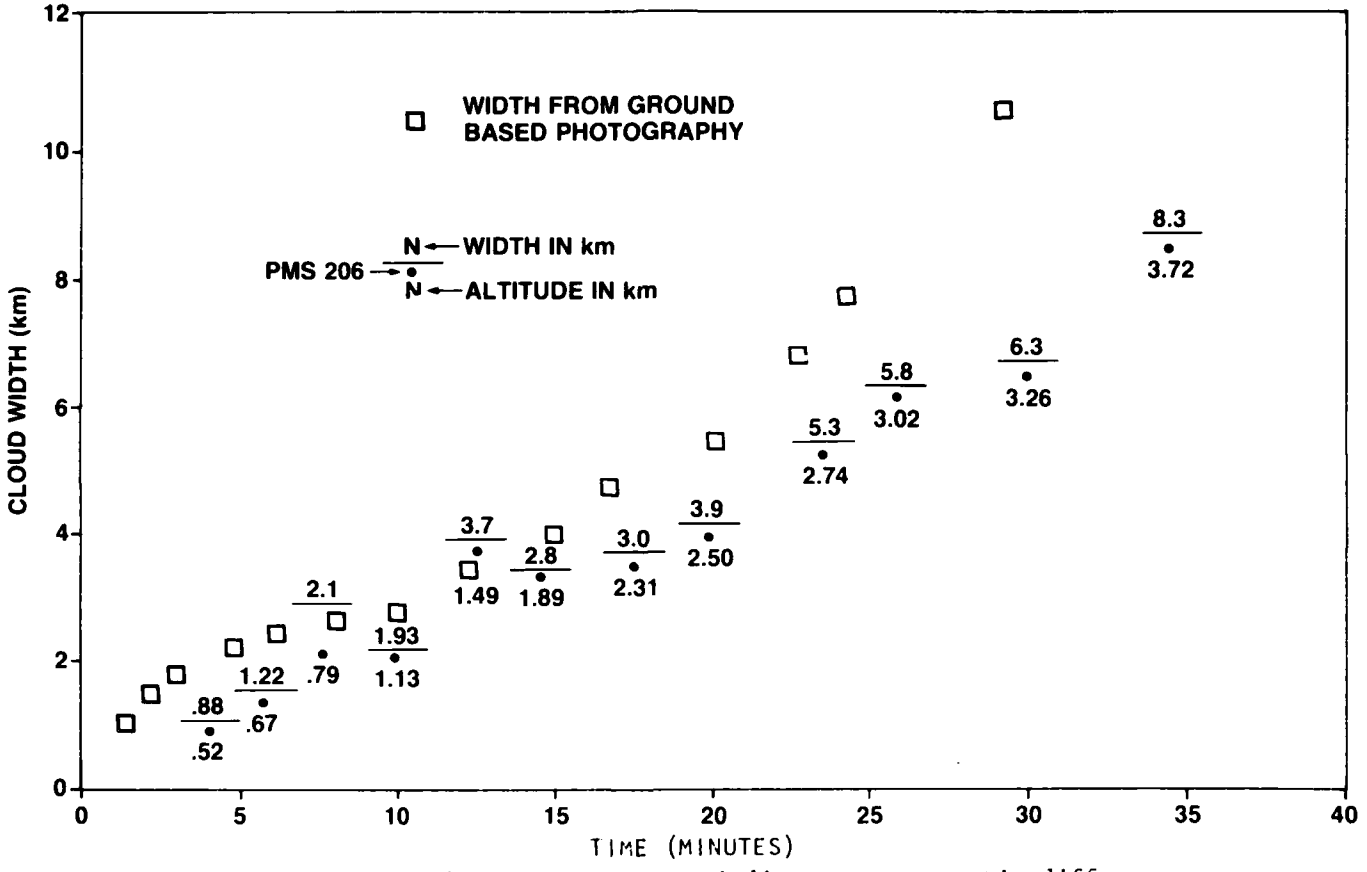

Figure 3.8. The above measurements indicate a systematic difference in cloud width measurement by the PMS 206 and that deduced from ground based photography at times later than T+15 minutes. (Analysis of photographic data furnished by Technology International Corporation).

and widths (as determined by time x velocity) to ±5% maximum.

For the purposes of illustrating the kinds of data processing and analysis provided, pass #6 of MISERS BLUFF II-2 was selected. This pass was approximately at the center of the cloud by our estimates and revealed a large statistical data set. Fig. 3.9 and 3.10 are computer generated time series plots for the FSSP/LAS-X combination and the two individual 2D probes.

The FSSP/LAS-X combination adequately covers the size range responsible for optical attenuation at visible wavelengths (extinction coefficients were computed at 600 nm in all work reported here). Plotted in Fig. 3.9 from bottom to top are four parameters; mass per unit volume or mass loading, concentration or number density, median volume diameter (MVD) and extinction coefficient. Both the mass loading and extinction coefficient change by orders of magnitude between in-cloud and out-of-cloud regions. The concentration changes by less than an order of magnitude due to the background contribution in the LAS-X lower channels of a few tenths of micron size. The MVD varies only by factors of 2 to 4 but shows large statistical fluctuations when out-of-cloud.

Fig. 3.10 shows time series plots for the individual 2D-C and 2D-P instruments. These series reveal the statistical quantization effects of 2D data record readout at two points in the pass. A continuous plot results only if the time between particles is resolved within records where data is sparce. These instruments show strikingly similar data signatures in the mass loading, concentration and MVD plots. The greatest difference is in the concentration which is approximately an order of magnitude higher for the 2D-C than 2D-P instruments (note the difference in scales, i.e., N cm^{-3} and N ℓ^{-1}). The MVD on the 2D-P probe is approximately 200 μm and, of course, cannot be less than 100 μm its lowest resolution value. The 2D-C probe MVD averages slightly over 100 μm which is the result of the added resolution below 100 μm. It is clear in comparing Figs. 3.9 and 3.10 that the average MVD must be between 20 and 200 μm. Adjusting for the difference in mass contributions between the two figures generates a value of approximately 50 μm.

PROCESSED DATA OUTPUT FOR PASS #6 OF MISERS BLUFF II-2
FOR THE LAS-X AND FSSP-100 COMBINATION

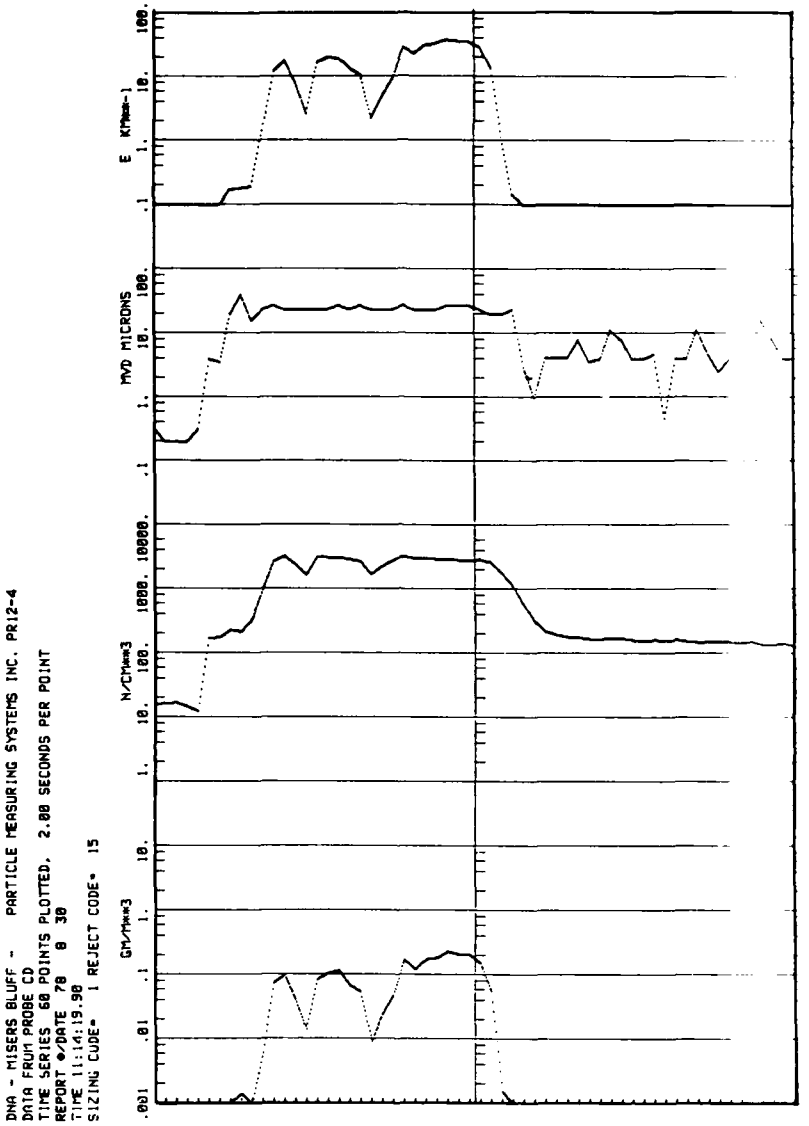

Figure 3.9. Time on the horizontal axis covers two minutes; the pass is about 50 seconds in width. The dust cloud is most easily defined in the extinction coefficient (top;km^{-1}), and mass loading (bottom;gm m^{-3}) plots. The concentration plot shows background amounting to 200 to 300 cm^{-3} when out-of-cloud contributed by the submicron size classes of the LAS-X. Mass loading has not been corrected for density (≈2.3 X too low in plot)

TIME SERIES PLOTS OF OAP-2D-C and OAP-2D-P DATA
FROM PASS #6 OF MISERS BLUFF II-2

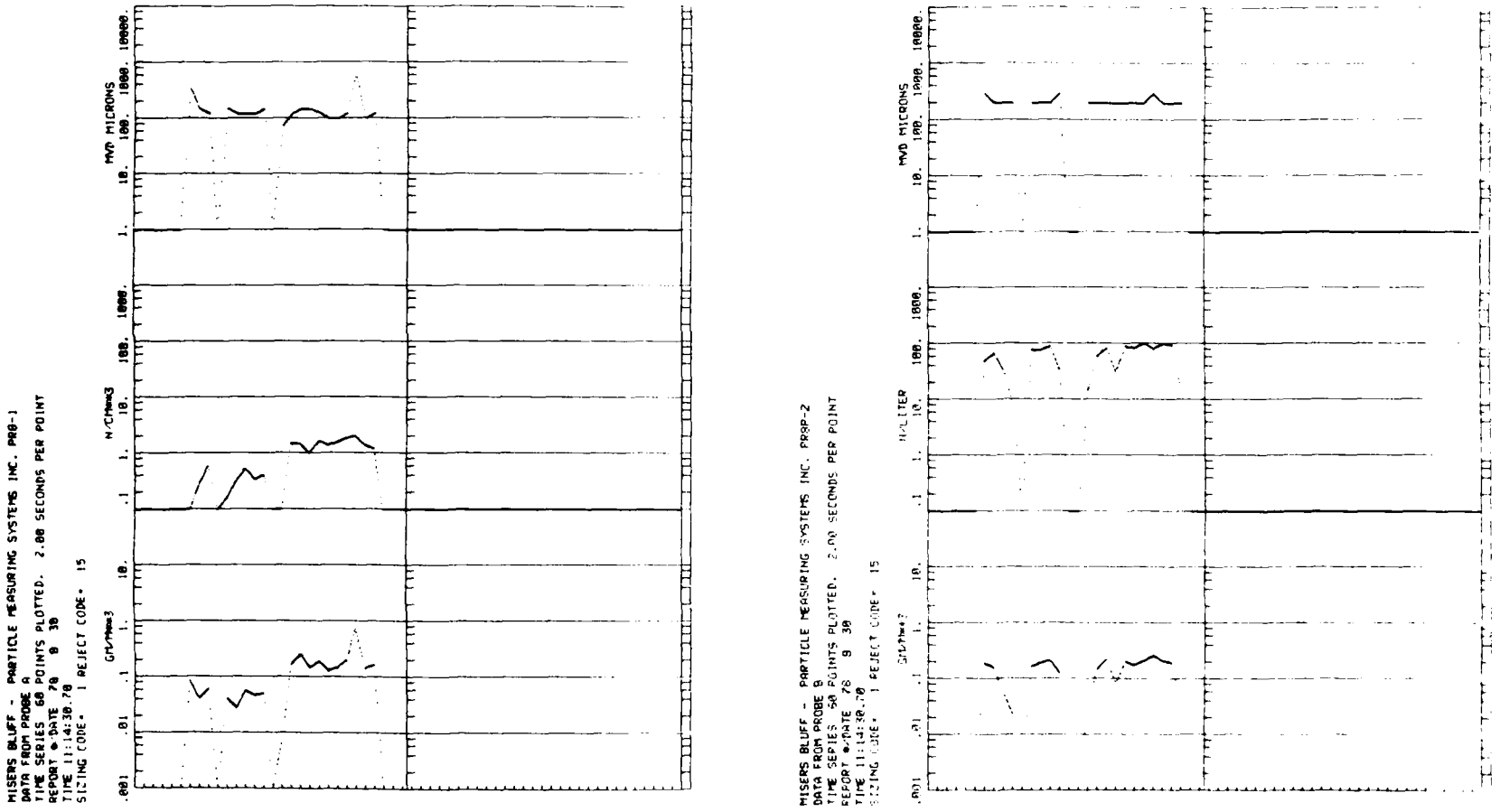

Figure 3.10. These data can be compared with that of Figure 3.7 but, in general, show similar signatures with the exception that regions of low concentration are exaggerated due to the quantization in data readout in the 2D probes. (For mass loading a value of $\rho = 1$ was used here).

Fig. 3.11, 3.12, and 3.13 show computer generated size and mass distributions for the FSSP/LAS-X combination and the individual 2D probes. The combined size distribution in Fig. 3.11 shows a smooth transition from the LAS-X to the FSSP probe and, in general, a fairly smooth power law fit ($n_r \sim r^{-3}$) between 1 and 10 μm. However, the mass distribution reveals the consequences of small changes in slope in the size distribution. In particular, the size distribution is bimodal with a small peak at 1 to 2 μm and a secondary much larger peak at 20 to 25 μm. It should be pointed out that the FSSP instrument is ordinarily calibrated for water droplets and the higher index soil particles generate reduced signal levels. Further signal loss due to contamination resulted. A 4 to 60 μm calibration was used for MISERS BLUFF II-2. With this adjustment the LAS-X and FSSP fit is quite good. However, one should be careful in using FSSP data above 30 μm. In that range irregular particles begin to scintillate due to specular reflections and refractions and the instrument is considerably less reliable than the 2D-C at larger sizes. More will be said in this regard later.

The 2D histograms in Fig. 3.12 and 3.13 show fairly steep exponential size distributions but much flatter mass distributions. In fact, the 2D-C mass distribution only begins to roll off noticeably at about 250 to 300 μm (eleventh size class). There is some evidence in the mass distribution for the 2D-P probe for a similar transition at about size class 3 (300 μm). The effects of statistical sample volume loss is apparent beyond 400 μm on the 2D-C probe and 1000 μm on the 2D-P probe. Note that the 2D-P instrument size distribution is below scale after size class three but the mass distributions for either probe will reflect single large particles and thus, the absence of a bar in the mass distribution is indicative of zero counts of that size.

A set of figures as given in Fig.3.9 - 3.13 exists for each pass in MISERS BLUFF II-1 and MISERS BLUFF II-2. Clearly, space does not permit their inclusion in this report. The reader is referred to the Quick Look Reports and final data submittal for details of various passes.

We should mention the fact that the 2D data was processed

SIZE (LEFT) AND MASS (RIGHT) DISTRIBUTIONS FOR THE
LAS-X AND FSSP-100 FOR PASS #6 MISERS BLUFF II-2

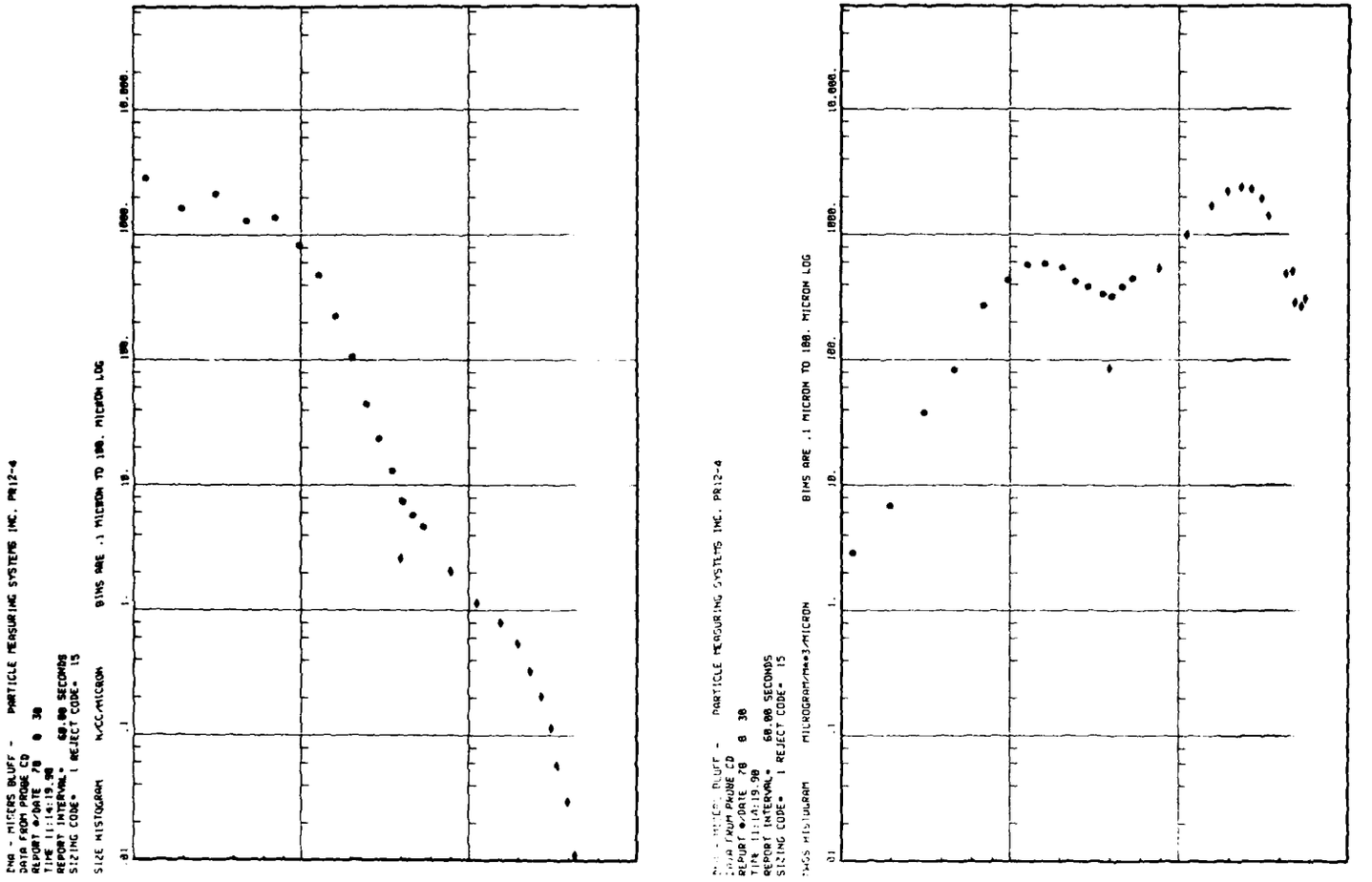

Figure 3.11. The fit between these two very different light scattering instruments is excellent. For various reasons the first channel of the FSSP often reads low and should be discarded in favor of the high resolution upper range of the LAS-X. The bimodal mass distribution is typical of many natural aerosol (5).

SIZE (LEFT) AND MASS (RIGHT) DISTRIBUTIONS FROM OAP-2D-C
PROBE OBTAINED DURING PASS #6 OF MISERS BLUFF II-2

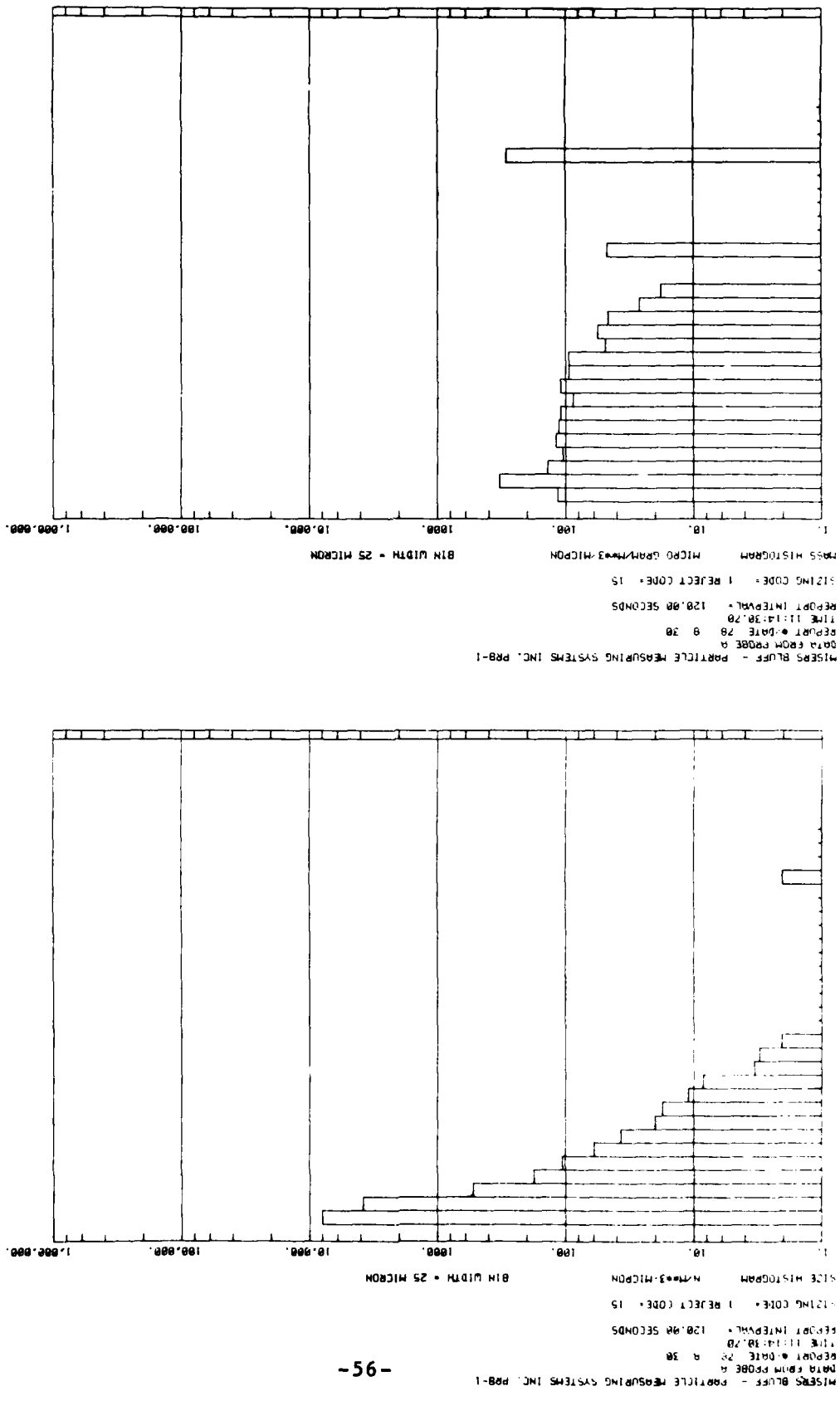

Figure 3.12

SIZE (LEFT) AND MASS (RIGHT) DISTRIBUTIONS FROM OAP-2D-P
PROBE OBTAINED DURING PASS #6 OF MISERS BLUFF II-2

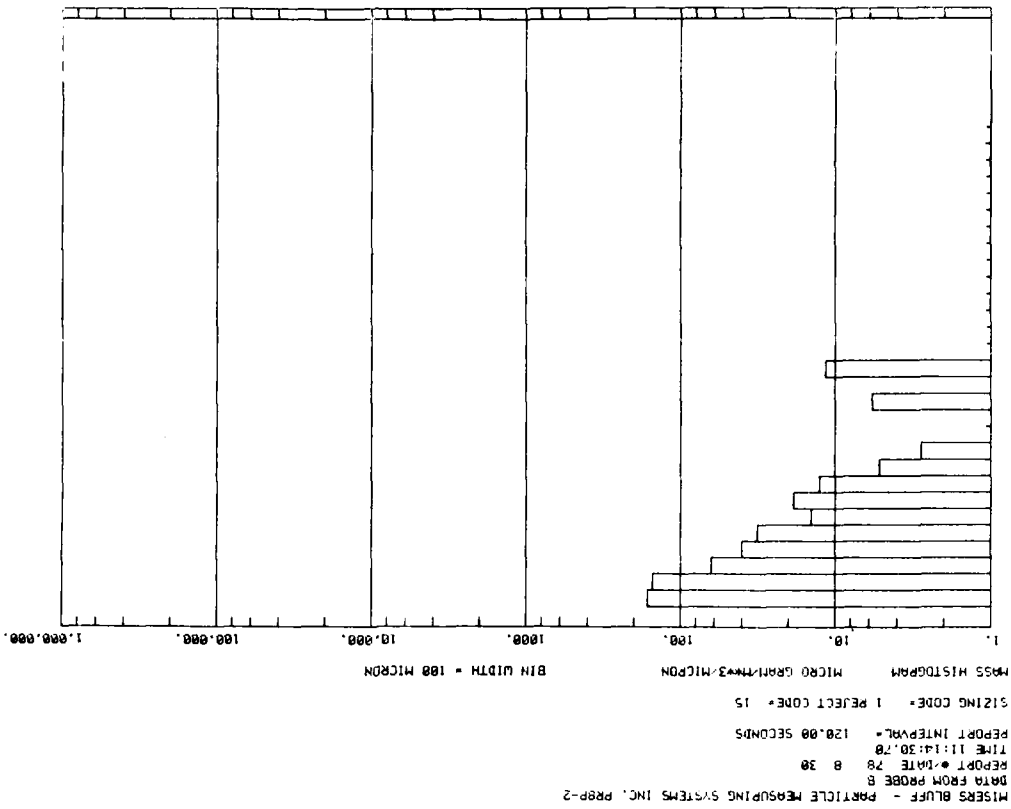

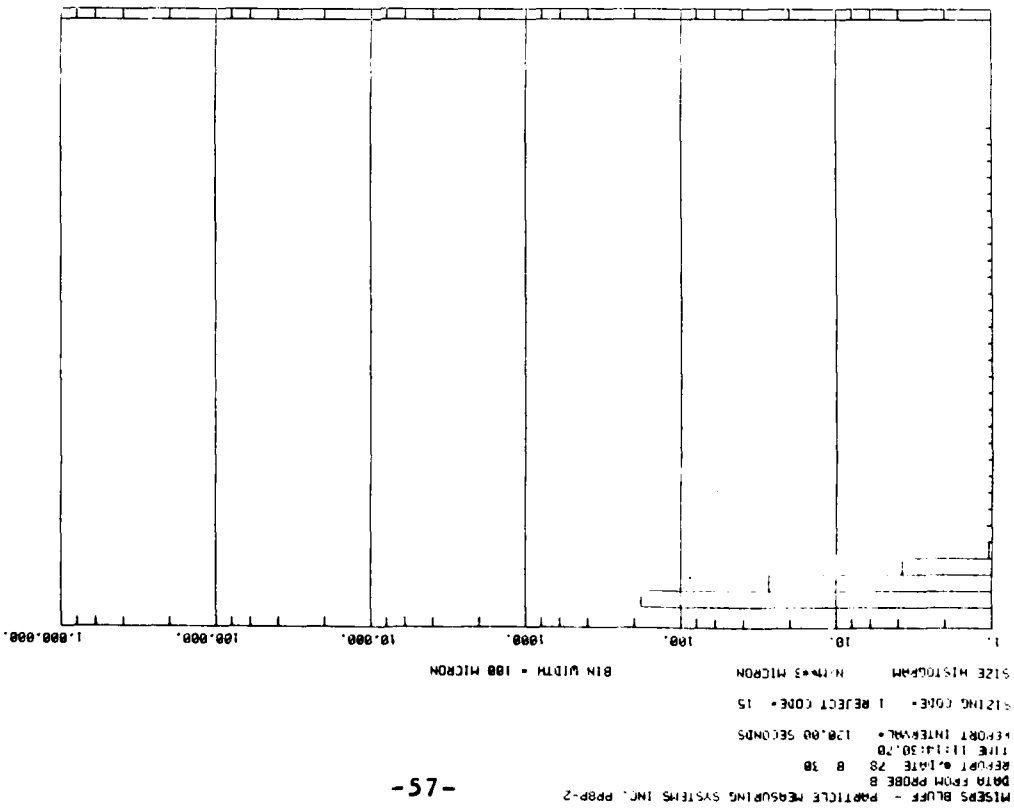

Figure 3.13

without partial image analyses. Fig. 3.14 illustrates raw imagery for the 2D probes. The reason that partial image analysis was not utilized is the presence of large organic particles that would erroneously bias towards higher mass values. Samples of organic materials are shown in Fig. 3.14. They are particularly obvious at later sampling times when soil particles of such size had long since fallen out. Because they extend beyond the array width the standard processing procedure on 2D data removes these organics. The organic materials observed in the 2D imagery were also collected on the PMS-206 oil soaked prefilter. Fig. 3.15 shows photographs of extracted samples from the filters of MISERS BLUFF II-1 and MISERS BLUFF II-2. A portion of the oil impregnated aircraft engine filter was scanned with a stereomicroscope (15X) to locate and measure the organic particles collected. Removal of the large particles for photographic documentation was no problem; however, most of the small ones (<2 mm) were quite friable, possibly a result of oil absorption, and not recoverable.

Utilizing the aircraft engine displacement, the typical rpm, and the seconds of time in the cloud, a total volume of cloud sampled by the aircraft engine filter was obtained with over twice as much cloud volume being sampled on MISERS BLUFF II-2 than on MISERS BLUFF II-1. In each case though, approximately two organic particles per cubic meter were detected by the filter.

These samples were categorized as to size (length) and the results presented in Fig. 3.16. The average concentration determined is only about 2 m^{-3}; however, the aircraft intake would hardly be isokinetic and it undoubtedly undersamples particles of such high drag/mass ratio. The 2D-P probe samples one cubic meter in about 10 seconds (sample volume is actually increased due to the large size of the particles) and thus, 2000 seconds of sampling would result in about 400 organics contaminating the 2D-P imagery. It is clear that the majority of these organics are rejected in 2D-C processing; however, some of the shorter ones are accepted by the 2D-P processing since they fit within the array width in certain orientations. Our own

IMAGERY SAMPLES FROM 2D PROBES

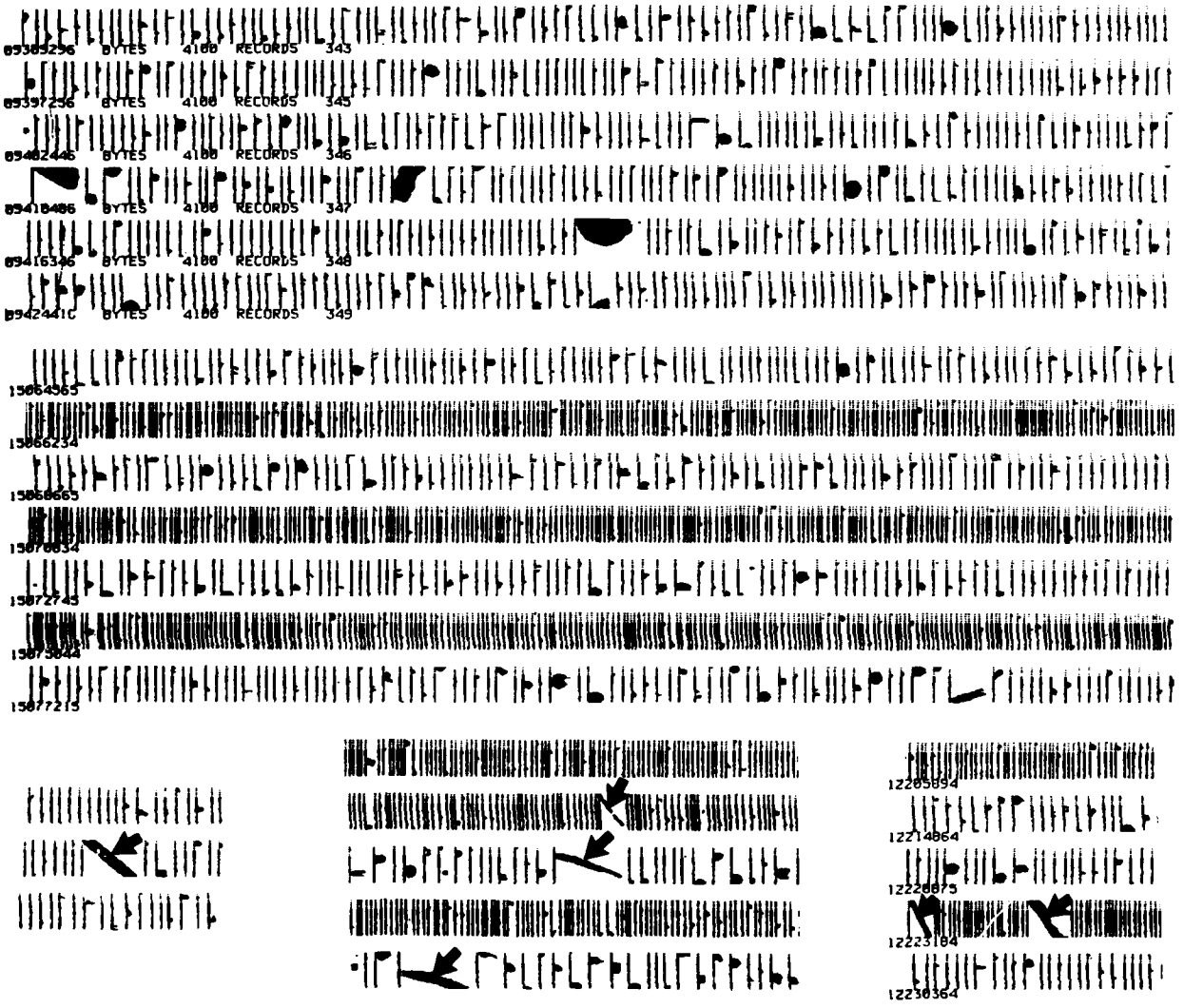

Figure 3.14. Raw imagery from OAP-2D-C of MISERS BLUFF II-1 (upper). Raw imagery from the OAP-2D-C and OAP-2D-P probes from MISERS BLUFF II-2 (middle). Images of organic materials (arrows) from selected 2D records in MISERS BLUFF II-1 and MISERS BLUFF II-2 (lower).

PHOTOGRAPHS OF ORGANIC MATERIALS EXTRACTED
FROM THE PMS 206 OIL SOAKED PREFILTERS

MISERS BLUFF II-1

MISERS BLUFF II-2

Figure 3.15

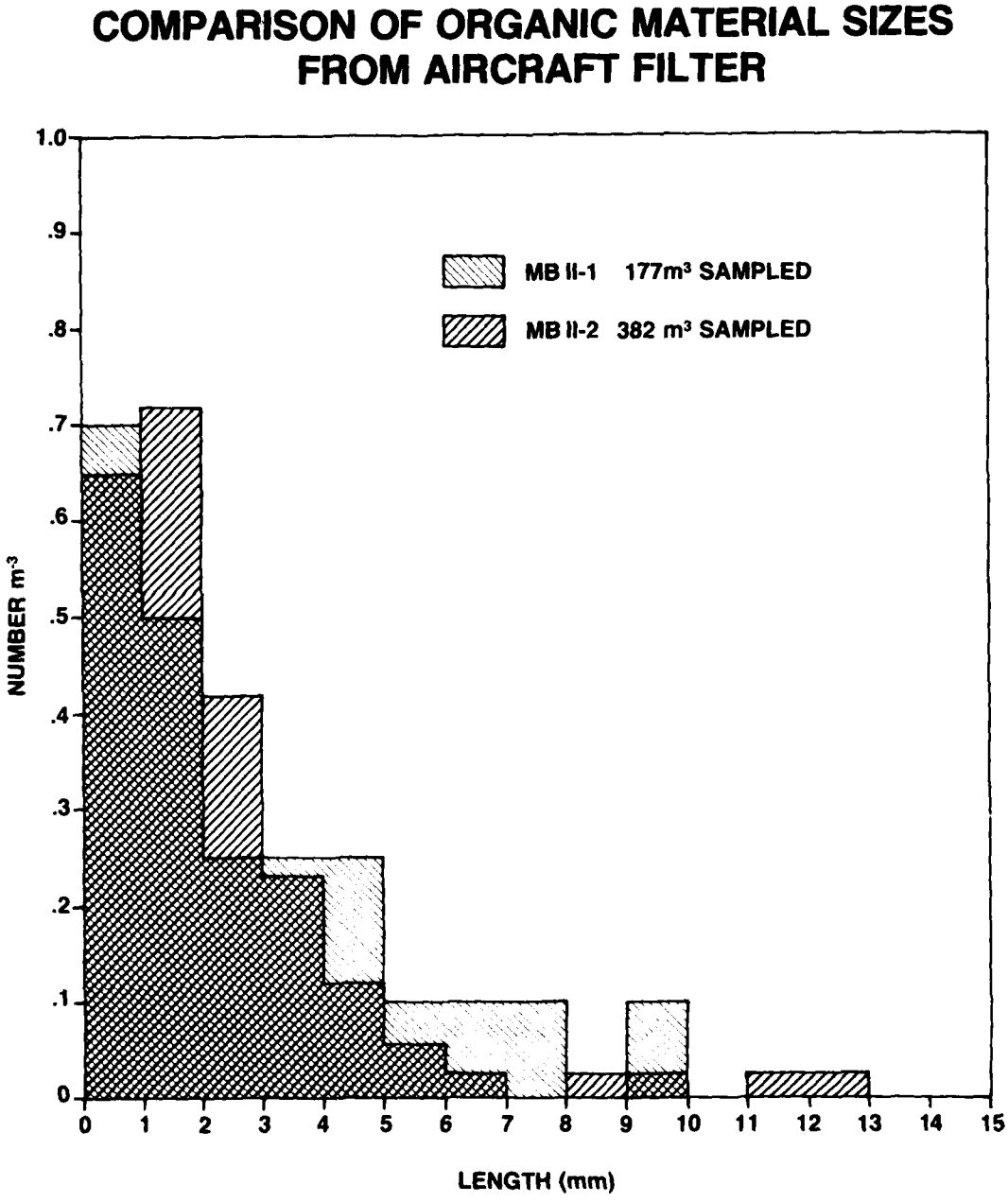

Figure 3.16: Size distribution of organic materials extracted from the PMS 206 oil soaked prefilter for MISERS BLUFF II-1 and MISERS BLUFF II-2. These organic materials were classified according to length and typically had aspect ratios greater than 4:1.

estimate is that they contribute to about a 5 to 10% overestimate of mass in the 2D-P probe. The error being largest at the latter sampling times.

In addition to the various pass analyses each entire flight was integrated for each probe to generate average size and mass distributions to intercompare various instruments. These are presented in Fig. 3.17 - 3.21. These curves average over in-cloud time and out-of-cloud time and include regions of known instrument anomalies. They still provide relative measures of intercomparison that are extremely valuable. The MISERS BLUFF II-1 size distribution of Fig. 3.17 is shown with the 200X, FSSP and 2D-C probes. The 200X probe shows somewhat higher values than the 2D-C probe which is really a sizing error and although systematic, is within general accuracy specifications. It is apparent here because of the steepness of the overall distribution. In general, the 2D-C data is considerably more accurate than that generated by the 200X not only because of its 2D characteristic, but because the OAP-200X used rectangular array elements on MISERS BLUFF II-1 (see Knollenberg[6]). The first channel of the 2D-C shows a large discrepancy as compared to the FSSP, exaggerated because of the steep slope in this region; this channel should be disregarded. The second channel of the 2D-C fits well with the FSSP data at its large end. The 2D-C distribution is generally quite smooth. The effects of statistical losses is again apparent above 400 μm.

The MISERS BLUFF II-2 size distribution data of Fig. 3.19 and 3.20 reveal excellent fits of the 2D-C and 2D-P data. With one exception the fit is equally good between the FSSP and 2D-C. The large end (50 to 60 μm region) of the FSSP appears to cut off abruptly in Fig. 3.19 for MISERS BLUFF II-2. This is caused by contamination of the FSSP optical system which affects the larger sizes greater because of the instrument's response (slope

of scattering signal vs. size).* The effect is exaggerated because the step-down passes were averaged with the step-up passes in this MISERS BLUFF II-2 data. The first channel of the 2D-C appears in better agreement with the FSSP. At sizes >∿40 μm the 2D-C must be used. The FSSP data in Figs. 3.18 and 3.21 show the characteristic mass mode at about 30 μm followed by a rapid decrease in mass at sizes above 40 μm. The mean (median size for MISERS BLUFF II-1 is about 90 μm (35 μm) while approximately 160 μm (42 μm) for MISERS BLUFF II-2.**

The AFTAC WC-135 aircraft also made particle size distribution measurements in the MISERS BLUFF II-2 dust cloud. We were able to obtain a sample of the filter material used to collect particles and photomicrographs of material collected are shown in Fig. 3.22. Comparative plots of relative size distributions measured by the WC-135 and PMS 206 are given in Fig. 3.23. The agreement is seen to be quite satifactory in the 20 to 100 μm range from pass #8 which is the closest pass to the sampling period of the WC-135 aircraft.

Fig. 3.22 also reveals small organic material particles; however, we were not able to find the large organic materials that were observed by the PMS 206. This may be due to their poor collection efficiency or shadowing affects from the large WC-135 fuselage envelope. In any case the relative agreement appears quite good in the size range we were able to analyze.

---

* Because of the measured higher level of contamination in MISERS BLUFF II-2 as compared to MISERS BLUFF II-1, the FSSP calibration for MISERS BLUFF II-2 of 4-60 μm and 4-48 μm for MISERS BLUFF II-1 were used in all final data processing.

The standard FSSP size range of 3-45 μm is for water droplets (m=1.33) and the higher index soil particles (m=1.5, m=1.6) require a systematic shift in calibration at sizes >12μm. However, this assumes that the particles are spherical. Non-spherical particles in certain orientations tend to produce scintillations and oversizing. Through microscopic examination of soil particles one also sees that the larger the particle the more varied its morphology. In effect, the two errors are partially compensating. Thus, we have estimated probable differences in calibration considering all effects (contamination, refractive index and particle morphology) gives rise to a size range of 4 to 48 μm for MISERS BLUFF II-1 and 4 to 60 μm for MISERS BLUFF II-2.

** The large difference in mean and median mass sizes is due to the sharp mass peak in the FSSP spectra. It is rather unusual but perhaps characteristic of explosively generated dust clouds.

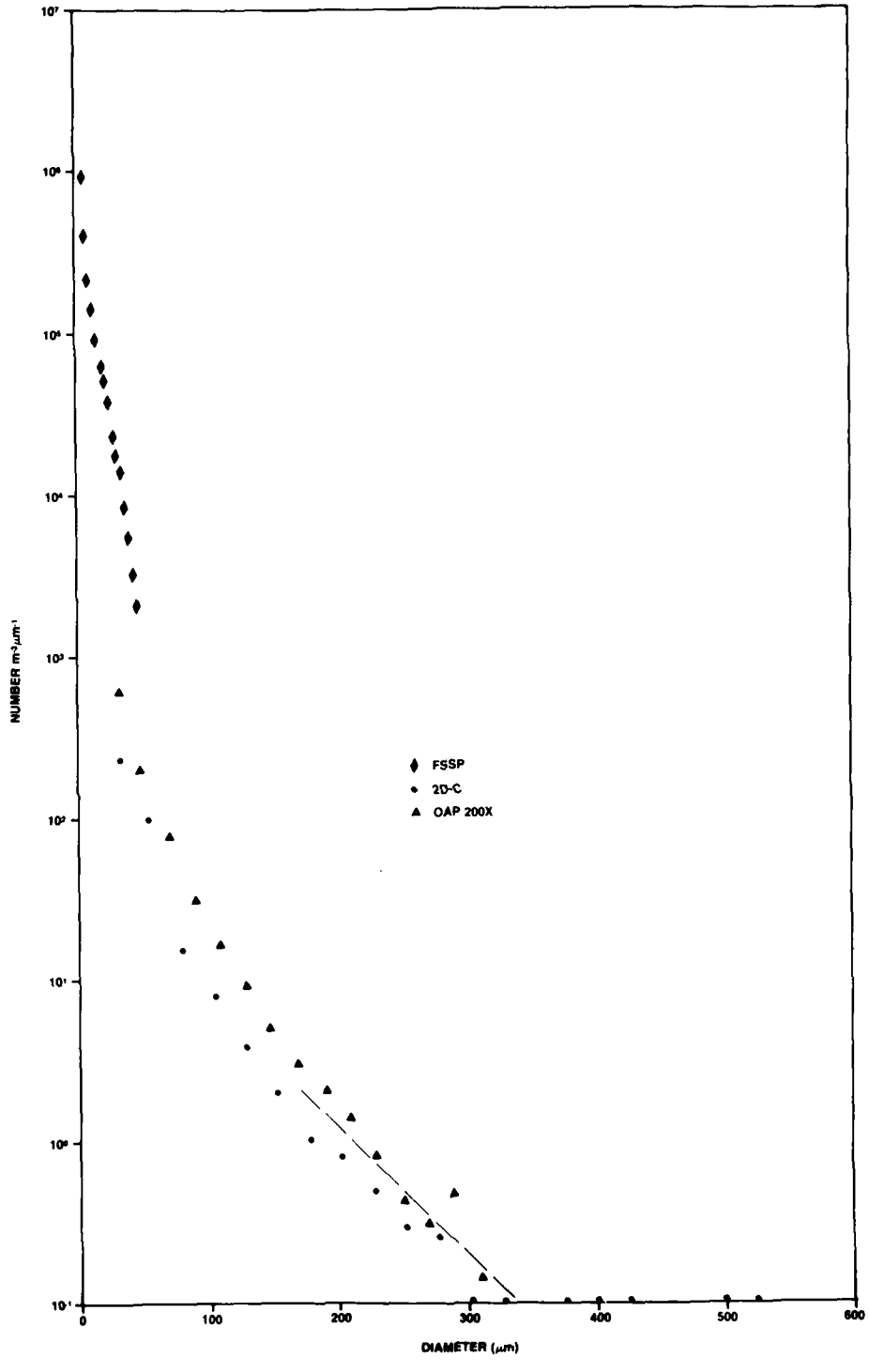

Figure 3.17: The OAP-200X data has been corrected for morphological effects. This requires increasing the measured size by approximately 30% over its entire range. The dashed line indicates a best fit of the OAP-2D-C data at sizes where sample volume is lost. Data points on the lower axis indicate no measurements of particles of that size.

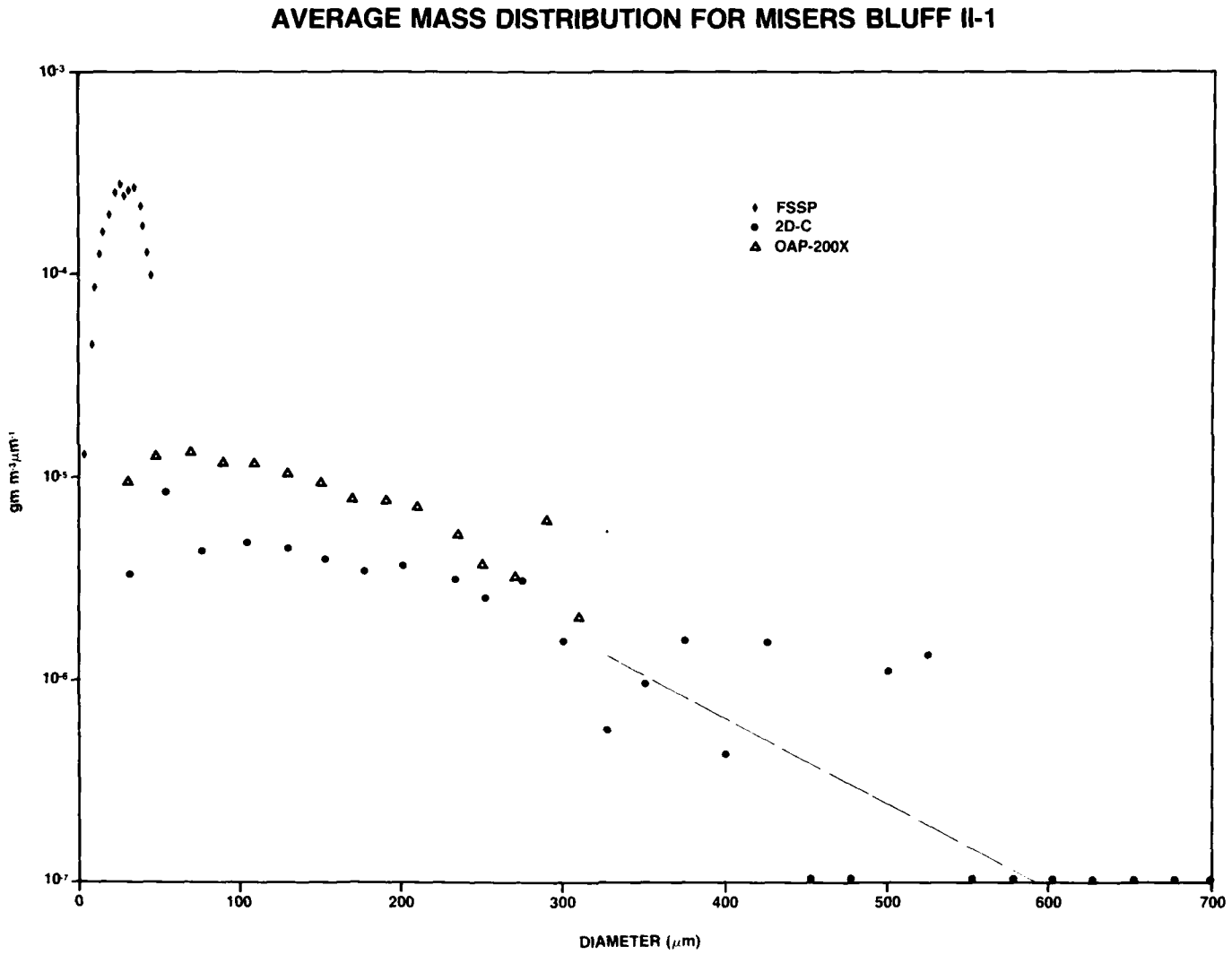

Figure 3.18: The dashed line indicates a best fit of the OAP-2D-C data at sizes where sample volume is lost. Data prints on the lower axis indicate no measurements of particles of that size.

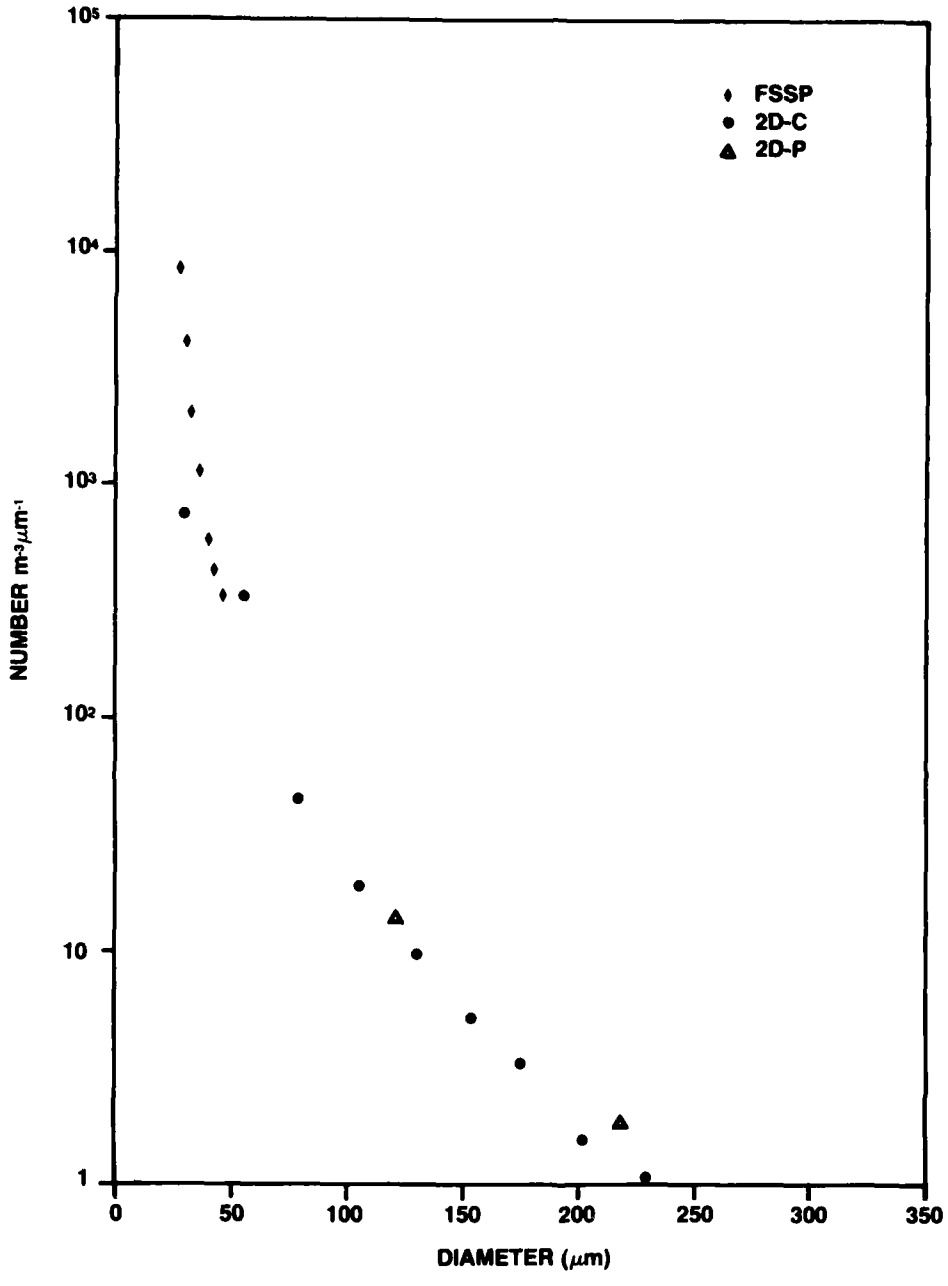

Figure 3.19: These data show the undersizing effects of the FSSP instrument at sizes larger than 40 μm (sizes smaller than 30 μm not plotted). We interpret this sharp cutoff to be the result of optical contamination which was concentrated near the center of the surface of the first collecting optical element which would effect larger sizes more strongly than small ones. The effect is exaggerated by the inclusion of passes later in the sampling mission. The 2D-C probe is not sensitive to such contamination and data from it are preferred at all sizes larger than 40 μm.

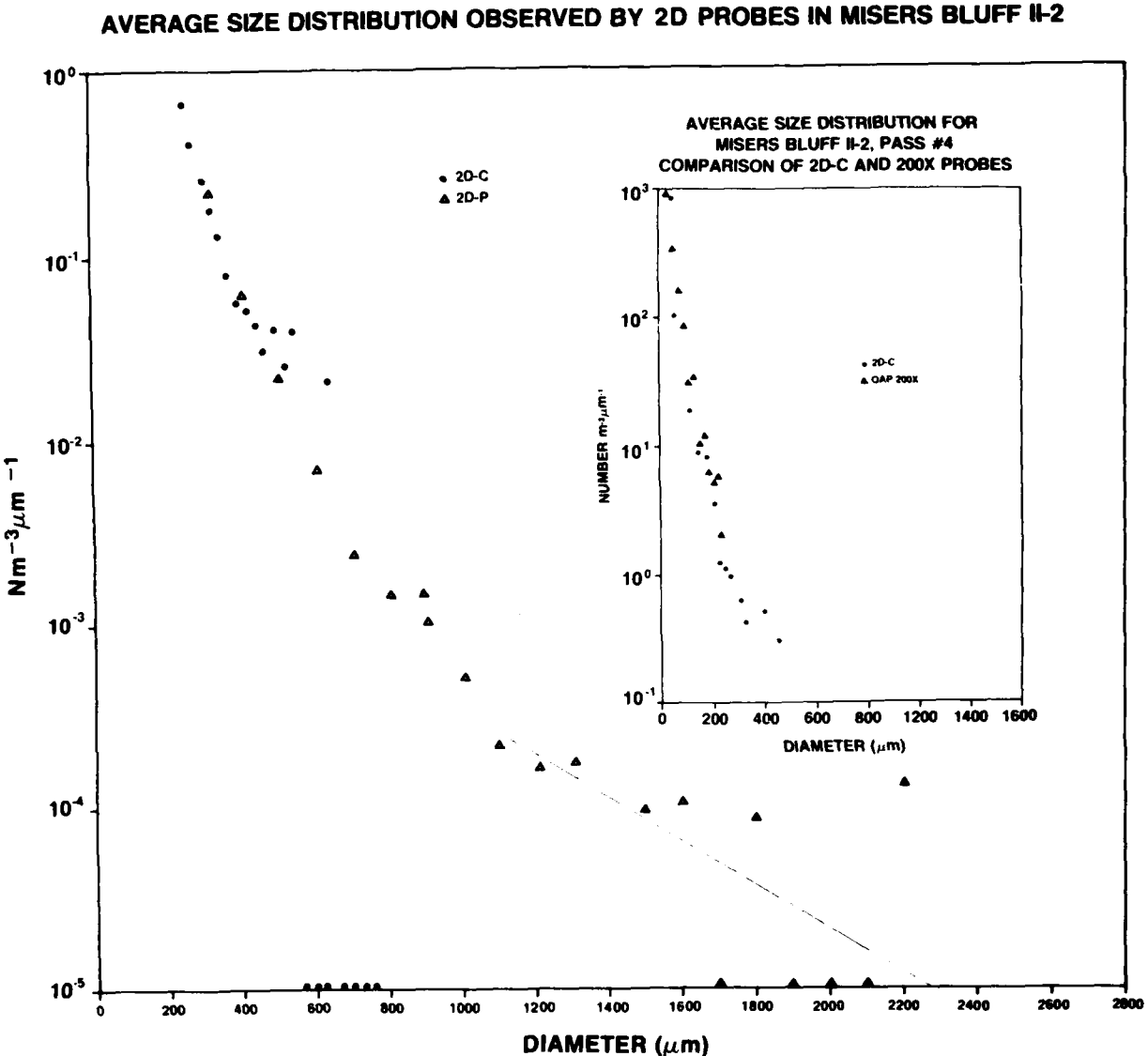

Figure 3.20: The dashed line indicates best fit of OAP-2D-P data at sizes where sample volume is lost. Data points on the size axis indicate no measurement of particles of that size. The insert shows a comparison of 2D-C and 200X data for one particular base. Note the excellent agreement when compared to Fig. 3.17 emphasizing the effect of array element geometry.

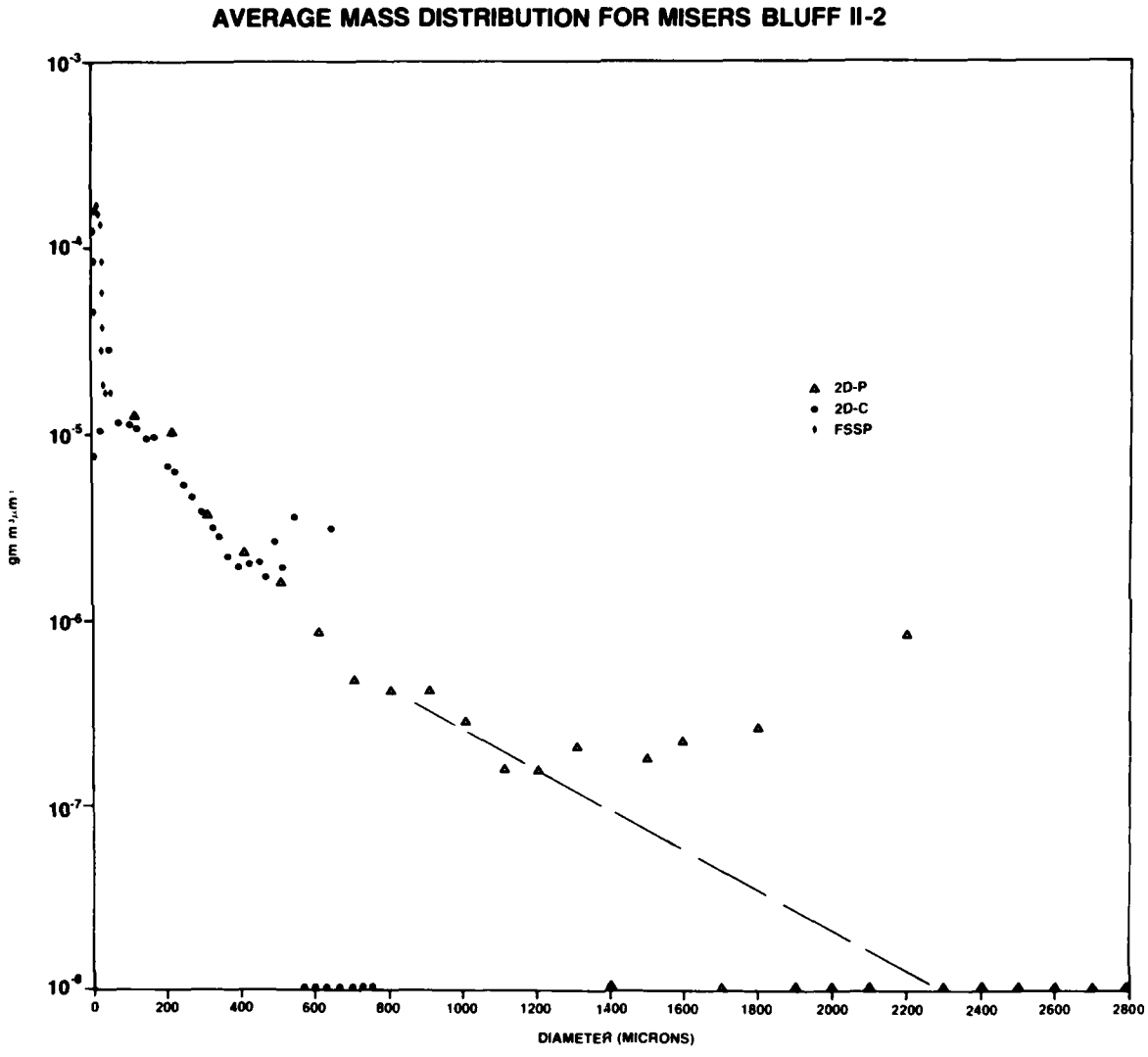

Figure 3.21: The data above includes the 2D-C, 2D-P, and FSSP instruments. The loss of sample statistics is apparent in the 2D-C instrument above 400 µm and above 1200 µm in the 2D-P instrument. Fortunately, the mass is concentrated at sizes where statistical sample losses can be ignored for the most part. Symbols for the 2D-P probe on the lower axis indicate that no particles were measured at those sizes.

PHOTOMICROGRAPHS OF MATERIALS EXTRACTED FROM WC-135 FILTERS

[——————————]
500 μm

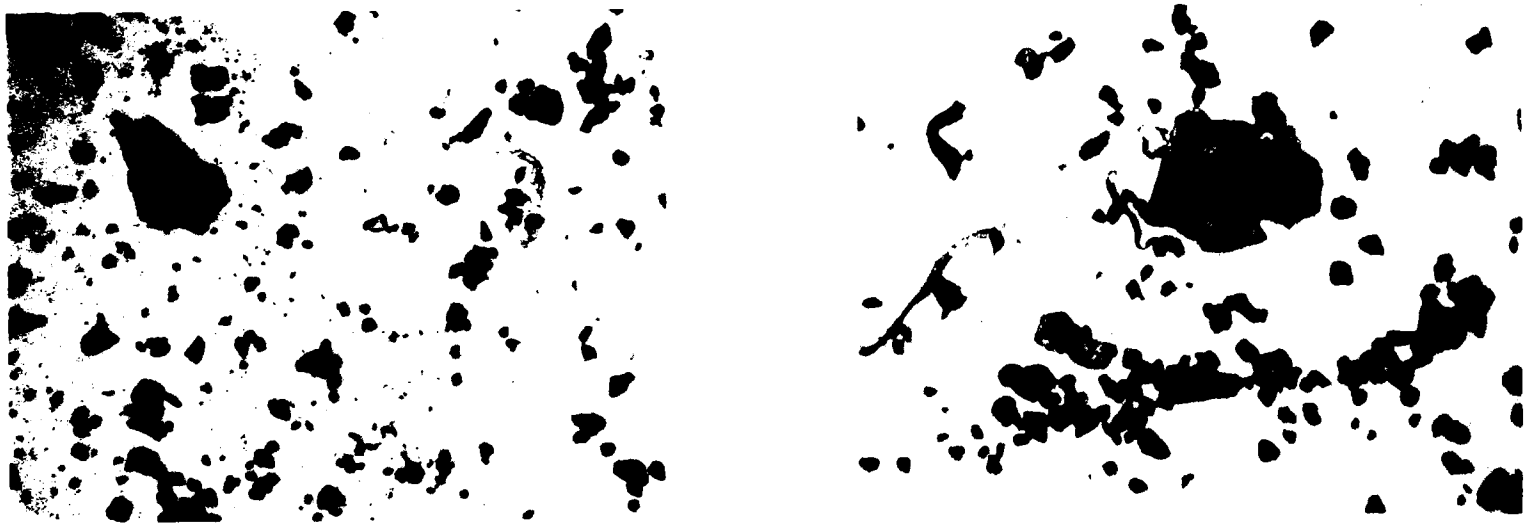

Figure 3.22. The presence of organic materials is also obvious in these samples although the large materials shown in Figure 3.15 were noticeably absent.

AFTAC WC-135 FILTER SAMPLE SIZE DISTRIBUTION
OAP-2DC RELATIVE COMPARISON

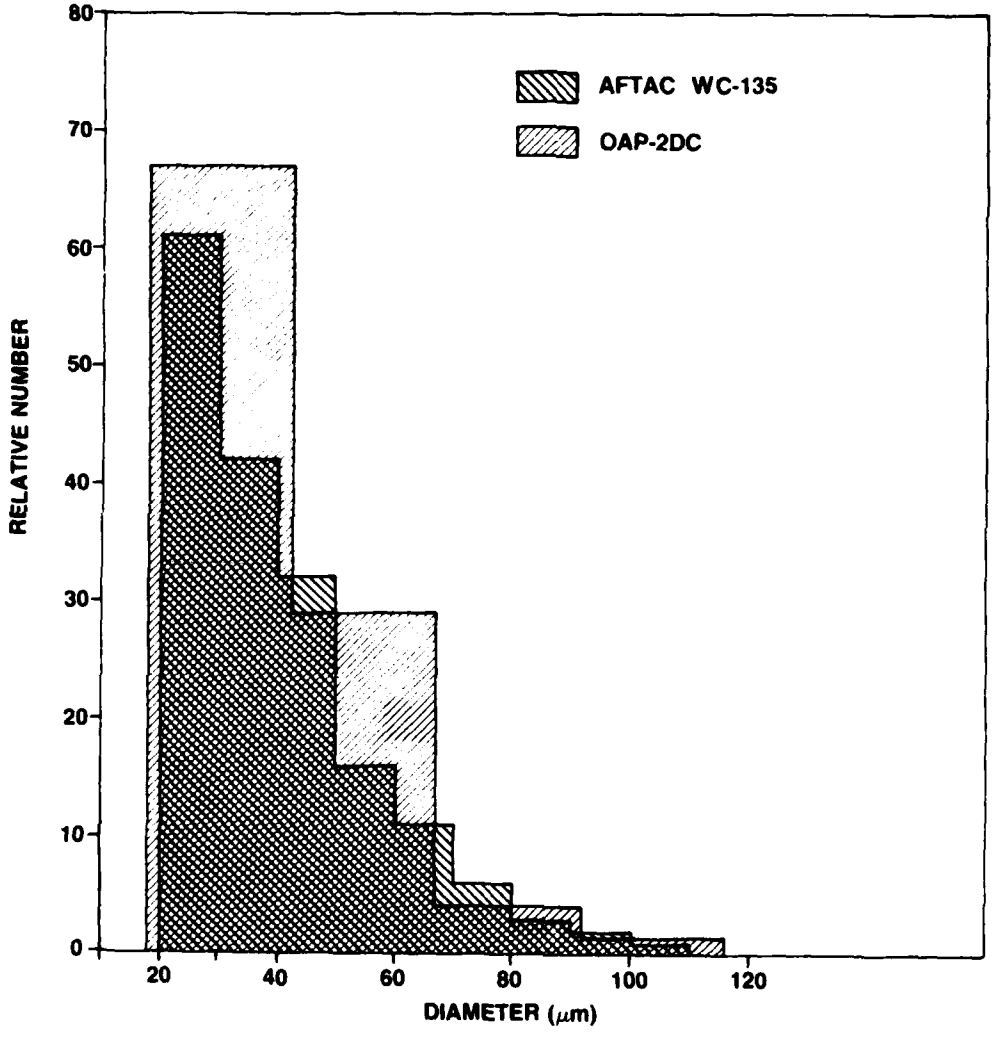

Figure 3.23: The above size distributions should be regarded as relative comparisons. The samples were actually taken at different times and the total relevant volume sampled by the WC-135 cannot be ascertained.

3.4 Discussion of Dust Cloud Mass and Optical Properties

Tables 3.1 and 3.2 also include a general summary of the MISERS BLUFF II-1 and MISERS BLUFF II-2 dust cloud mass and optical properties. The mass values are computed using the measured fines density of the soil samples of 2.29 gm cm^{-3}. The optical values are all computed at 0.63 μm wavelength. The integration of mass loading over a horizontal cylindrical slice 1 m thick for each pass provides a relative measure of mass as a function of altitude. This parameter is designated as the cross sectional mass loading in Tables 3.1 and 3.2. The extinction coefficient (EXCO) is computed from MIE theory, the visibility from the visibility relationship where $V = \frac{3.94}{EXCO}$, and the optical depth is the product of EXCO x WIDTH. Additional parameters summarized are the maximum size from the 2D probes, peak values of EXCO and minimum visibility values.

The greatest mass lofted was by MISERS BLUFF II-2 (5.23 Mkg) as compared to MISERS BLUFF II-1 (0.80 Mkg). These values were determined by integrating the cross sectional mass loadings through the clouds' vertical depths. The ratio of mass lofted for these clouds MISERS BLUFF II-2/MISERS BLUFF II-1 is 6.6. The highest average mass loading was observed on pass #3 of MISERS BLUFF II-1 where 0.67 gm m^{-3} was measured. The highest average mass loading observed for MISERS BLUFF II-2 was on pass #6 where 0.41 gm m^{-3} was measured. MISERS BLUFF II-2 had larger particles as revealed by the increase in mean mass size (160 μm as compared to 90 μm) and observations of largest particles listed in Tables 3.1 and 3.2.

A summary of the mass properties in MISERS BLUFF II-2 is given in Fig. 3.24 where the largest particle observed, cross sectional mass loading, and accumulative mass loading are plotted as functions of altitude. Comparisons of cross sectional mass loading and the largest particle observed are rather revealing. While the cross sectional mass loading increases with height up to about 2.5 km and then decreases, the largest particle observed reads a maximum at low level and then steadily decreases. This verifies that the largest particles are not important to the mass loading at the time the PMS 206 measurements were made. We,

SUMMARY OF MISERS BLUFF II-2 PARTICLE MASS PROPERTIES

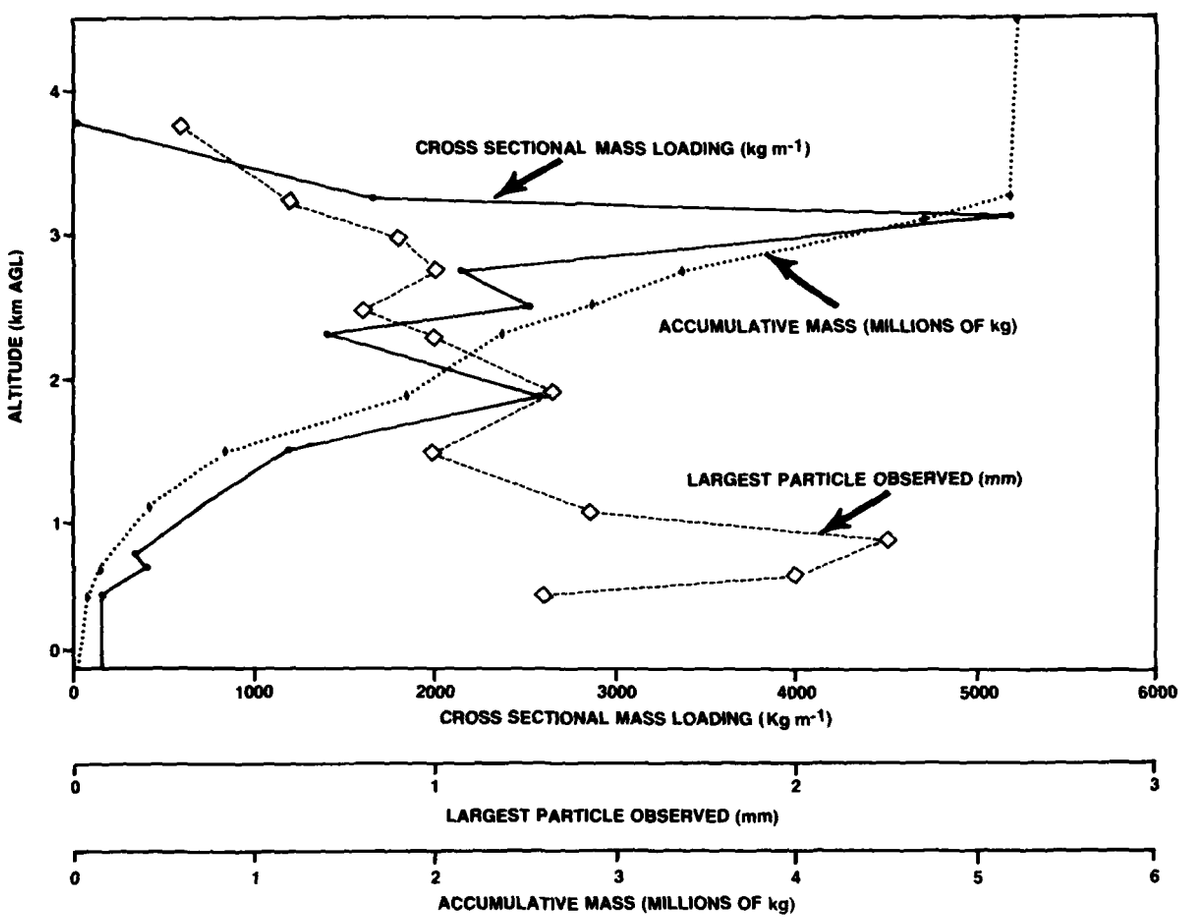

Figure 3.24

of course, previously observed this in the mass distributions presented. It furthers our confidence in having covered the size ranges of importance adequately.

It is also instructive to go back and compare the size and mass distributions measured in these clouds with the soil sample size and mass distributions of Fig. 2.3 and 2.4. While the size distributions are strikingly similar the mass distributions of Fig. 2.4 reveal a mass peak at about 200 μm that wasn't observed during the airborne measurements. However, the characteristic change in slope at 250 to 300 μm is evident. We believe the differences between these distributions are in reality due to the presence of increased small particle production in the 20 to 200 μm size range by the MISERS BLUFF II-1 and MISERS BLUFF II-2 events. Some of the very small particles here could be combustion products; a more likely effect at sizes of 100 μm would be the lack of coagulation effects present in the ground sample. At still larger sizes the slope is slightly steeper in the airborne data which may be due to sedimentation effects; however, we were surprised by the small influence of sedimentation. We were still observing 300 μm particles an hour after detonation on MISERS BLUFF II-2.

The optical properties of these events were also of considerable interest. One surprising result was that the maximum optical depth was observed at a much lower altitude on MISERS BLUFF II-1 than MISERS BLUFF II-2. A second surprise was the percentage of the optical depth that was in the FSSP size range. Fig. 3.25 shows a comparison of the extinction coefficient time series for pass #6 of MISERS BLUFF II-2 with and without the LAS-X. The difference is seen to be about 60%. Passes #4, 5, 11 and 12 of MISERS BLUFF II-2 were actually corrected by use of the printed LAS-X data to fill in the LAS-X contribution missing. More importantly, the MISERS BLUFF II-1 data wherein only the FSSP was used is probably low by about the same 60%. The maximum optical depth on MISERS BLUFF II-1 was 30.2 as compared to 45.9 on MISERS BLUFF II-2. Minimum measured visibilities were similar in both clouds (∿100 meters); however, the average

EXTINCTION COEFFICIENT PLOTS FOR PASS #6

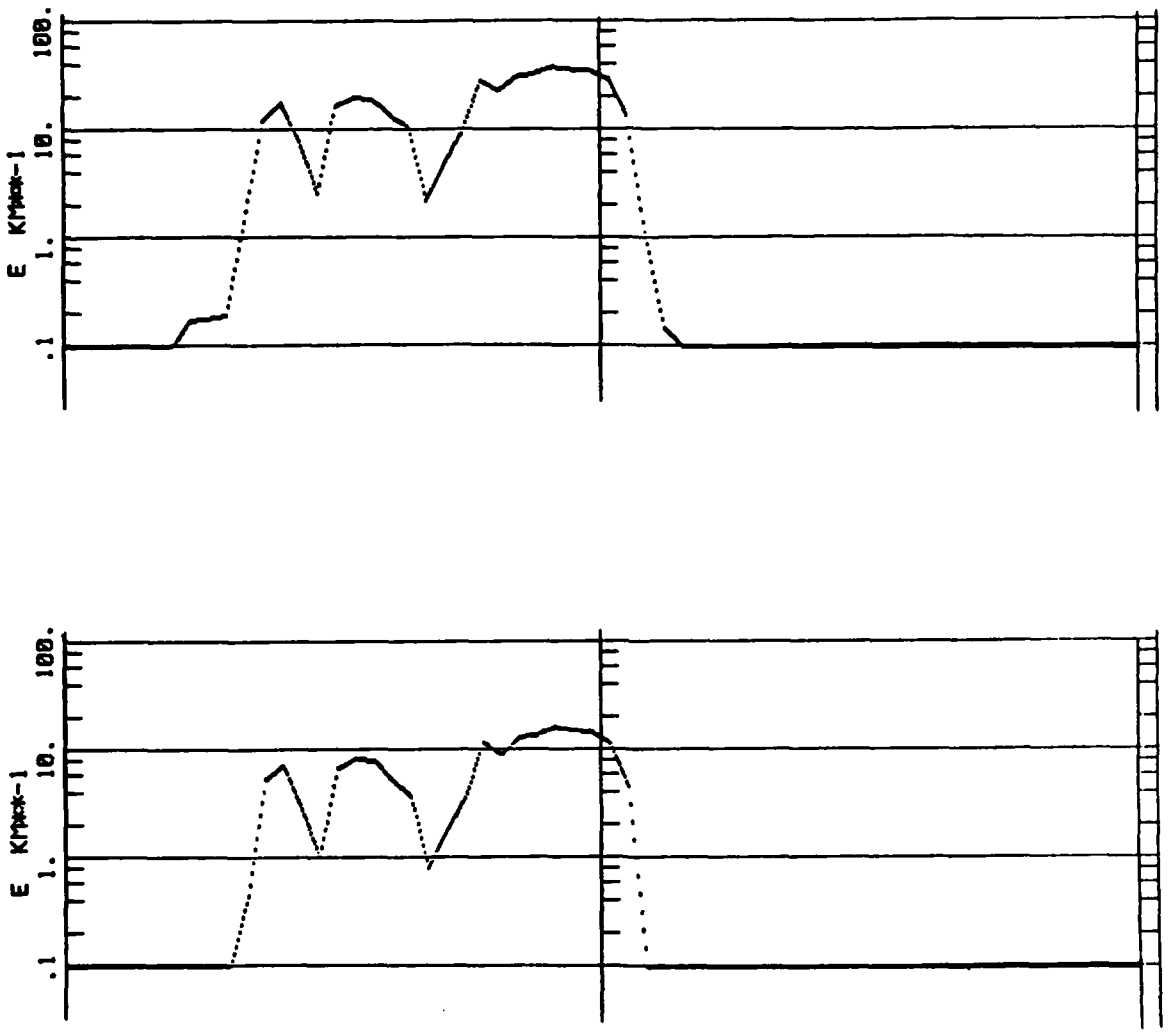

Figure 3.25. The top plot is for both FSSP and LAS-X instruments while the bottom plot is for the FSSP alone. This comparison indicates that the ratio of contributions from the LAS-X and FSSP divides nearly equally.

minimum visibility was less (and mass loading greater) on pass #3 of MISERS BLUFF II-1 than any pass on MISERS BLUFF II-2.

The fact that nearly one-half of the optical particle cross section is in the FSSP size range leads us to believe that these particles are not direct combustion products but indeed fine soil particles. This confirms our use of 1.5-1.6 refractive index values with a corresponding size range of 4 to 60 μm for the FSSP. The LAS-X has no systematic shift in size calibration associated with real refractive index (sensitive only to absorption), thus providing an indication of refractive index when compared to the FSSP in the region of size range overlap. Suffice to say the agreement is much better when an FSSP calibration of 4 to 60 μm is used on MISERS BLUFF II-2.

4.0 CONCLUSIONS

In terms of the analyses we chose to perform, it would appear that the MISERS BLUFF II-1 and MISERS BLUFF II-2 dust clouds were sampled with considerable success. Not only is the data base sufficient to characterize the mass properties of both clouds, it also appears quite sufficient to characterize the clouds optically.

One obvious conclusion drawn is that the mass of dust lofted does appear to be nearly linearly related to the HE yield. The six fold HE increase of MISERS BLUFF II-2 over MISERS BLUFF II-1, in fact, yielded nearly a 6.6 fold increase in lofted mass. One can also categorically state that the larger particles are not responsible for the bulk of the mass. At least not at the times our measurements were made. The average mass loading observed through the first ten to twenty minutes is typically a few tenths of a gram and the mean mass size is about 100 to 150 μm.

We were also surprised at the overall lack of particles of a few millimeters size. We were led to believe that there would be some there and on MISERS BLUFF II-1 were set up to cover up to 6 mm. The largest non-organic particle observed on MISERS BLUFF II-1 and MISERS BLUFF II-2 were 1.25 mm and 2.25 mm respectively. The largest particles observed on MISERS BLUFF II-2 were in the first pass. These were polyparticles or aggregates, which resulted in noisy impacts on the windscreen but because of their friability created no damage.

In terms of optical effects at visible wavelengths the attenuation is largely at sizes of about 5 μm. One would, in fact, expect to see considerable attenuation at infra-red wavelengths. Conversely at the times our measurements were made the attenuation at microwave frequencies should be very small except perhaps at near millimeter wavelengths.

Our data analyses also support the important fact that the relative distribution of dust clouds generated by HE events can be estimated from ground samples.

In terms of future operations it is clear that HE generated dust clouds can be sampled safely. We were surprised at the

lack of turbulence in the clouds at early sampling times. The greatest hazard is in dust injestion to the engine. The engine wear factor is directly proportional to exposure. Our total time in-cloud was obviously much longer than prior work and even though precautions were taken noticeable wear resulted. Based on our experience an upper limit of 1800 seconds of in-cloud sampling time is the maximum that one would consider as a safe upper exposure limit. It would also seem desirable to have a better filtration system for the engine intake. This would require certain modifications but would be straightforward.

The fact that we were able to use our own aircraft prefilter as an important data sample source leads us to believe that a filter sampler would greatly enhance the overall data. A sequential filter sampler(pod mounted) is currently being fabricated at PMS and should be available for future work.

Overall the cloud concentrations are very similar to natural terrestrial clouds except for the more highly concentrated submicron region. Thus, instruments designed for cloud physics work are largely suitable. At 0.1 μm the concentration is less than an order of magnitude above background. We believe our estimates of total mass lofted to be within $^{+50}_{-30}$% and optical properties evaluated to ±25%. The mass error may likely be an underestimate for three reasons; loss of sampling large particles at early times and while out-of-cloud and the fact that our 2D probes were mounted in horizontal rather than vertical orientations. Thus, if particles had shape factors to allow for preferred orientations our measurements would be biased to the smaller dimensions. Examination of some of the PMS 206 and WC-135 materials collected shows certain platelike minerals that might well be stably oriented during freefall. In future work crossed orientations of two identical instruments would be particularly useful.

Finally, our analysis is truly an overview. There remains the task of looking at the data at high spatial resolution and the analysis of the in-cloud variability with regard to various parameters. Also comparisons of samples at the same altitudes but at

different times could be invaluable in estimating cloud volumetric changes. Further analysis should be conducted to maximize the usefulness of the data set provided.

REFERENCES

1. Proceedings of the Dice Throw Symposium, 21-23 June, 1977, Sponsored by the Defense Nuclear Agency Contract No. DNA 001-75-C-0023, Washington, D.C., July 1977.

2. Green, W. D. and M. J. Fegley, "Analysis of Aerosols and Fallout From High-Explosive Dust Clouds", Technical Report Meteorology Research, Inc., Altadena, California, March 3, 1977.

3. Knollenberg, R. G., "The Optical Array: An Alternative to Extinction and Scattering for Particle Size Measurement", J. Appl. Meteor., Vol. 9, No. 1, 1970.

4. Knollenberg, R. G., "Three New Instruments for Cloud Physics Measurements: The 2-D Spectrometer, The Forward Scattering Spectrometer Probe, and The Active Scattering Aerosol Spectrometer", A. Meteor. Society, International Conference on Cloud Physics, July 26-30, 1976, Boulder, Colorado, pp 554-561.

5. Whitby, K. T., and G. M. Sverdrup, "California Aerosols: Their Physical and Chemical Characteristics", University of Minnesota, Particle Technology Lab Publication No. 347, Spring, 1978.

6. Knollenberg, R. G., "The Response of Optical Array Spectrometers to Ice and Snow: A Study of 2-D Probe Area-to-Mass Relationships", Final Report March 22-June 30, For Air Force Geophysics Lab, AFGL-TR-76-0273, Nov. 8, 1976.

DISTRIBUTION LIST

DEPARTMENT OF DEFENSE

Assistant to the Secretary of Defense
Atomic Energy
ATTN: Executive Assistant

Defense Advanced Rsch. Proj. Agency
ATTN: TIO

Defense Communications Agency
ATTN: CCTC

Defense Technical Information Center
12 cy ATTN: DD

Defense Intelligence Agency
ATTN: DT-2, T. Dorr
ATTN: DT-2
ATTN: DB-4D
ATTN: DT-1C

Defense Nuclear Agency
ATTN: RATN
ATTN: SPSS
ATTN: SPTD
ATTN: STSP
ATTN: STVL
ATTN: DDST
2 cy ATTN: SPAS
4 cy ATTN: TITL

Field Command
Defense Nuclear Agency
ATTN: FCTMOF
ATTN: FCTMO
ATTN: FCPR
ATTN: FCTMOT

Field Command
Defense Nuclear Agency
Livermore Division
ATTN: FCPRL

Joint Chiefs of Staff
ATTN: SAGA/SFD
ATTN: SAGA/SSO
ATTN: J-5, Force Planning & Program Div.
ATTN: J-5, Nuclear Division

Joint Strat. Tgt. Planning Staff
ATTN: JPST, G. Burton
ATTN: JPST
ATTN: JPTM
ATTN: JLTW-2

NATO School (SHAPE)
ATTN: U.S. Documents Officer

Undersecretary of Def. for Rsch. & Engrg.
ATTN: Strategic & Space Systems (OS)
ATTN: Engineering Technology, J. Persh

DEPARTMENT OF THE ARMY

BMD Advanced Technology Center
Department of the Army
ATTN: ATC-T, M. Capps

DEPARTMENT OF THE ARMY (Continued)

BMD Systems Command
Department of the Army
ATTN: BMDSC-H, N. Hurst
ATTN: BMDSC-HW, R. Dekalb

Deputy Chief of Staff for Ops. & Plans
Department of the Army
ATTN: DAMO-NCZ

Deputy Chief of Staff for Rsch. Dev. & Acq.
Department of the Army
ATTN: DAMA-CSS-N

Harry Diamond Laboratories
Department of the Army
ATTN: DELHD-N-TF
ATTN: DELHD-N-P
ATTN: DELHD-N-P, J. Gwaltney

U.S. Army Ballistic Research Labs
ATTN: DRDAR-BLV, W. Schuman, Jr.
ATTN: DRDAR-BL, R. Eichelberger
ATTN: DRDAR-BLT, R. Vitali
ATTN: DRDAR-BLV
ATTN: DRDAR-BLT, J. Frasier
ATTN: DRDAR-BLE, J. Keefer

U.S. Army Material & Mechanics Rsch. Ctr.
ATTN: DRXMR-HH, J. Dignam

U.S. Army Materiel Dev. & Readiness Cmd.
ATTN: DRCDE-D, L. Flynn

U.S. Army Missile R&D Command
ATTN: DRDMI-XS
ATTN: DRDMI-TRR, B. Gibson
ATTN: DRDMI-TKP, W. Thomas

U.S. Army Nuclear & Chemical Agency
ATTN: Library

U.S. Army Research Office
ATTN: P. Radowski, Consultant

U.S. Army TRADOC Systems Analysis Activity
ATTN: ATAA-TDC, R. Benson

DEPARTMENT OF THE NAVY

Naval Research Laboratory
ATTN: Code 2627
ATTN: Code 7908, A. Williams
ATTN: Code 6770, G. Cooperstein

Naval Sea Systems Command
ATTN: SEA-0352, M. Kinna

Naval Surface Weapons Center
ATTN: Code R15, J. Petes
ATTN: Code F31
ATTN: Code K06, C. Lyons

Naval Weapons Evaluation Facility
ATTN: P. Hughes
ATTN: L. Oliver

DEPARTMENT OF THE NAVY (Continued)

Office of Naval Research
ATTN: Code 465

Office of the Chief of Naval Operations
ATTN: OP 604C
ATTN: OP 604C3, R. Piacesi
ATTN: OP 604E14, R. Blaise

Strategic Systems Project Office
Department of the Navy
ATTN: NSP-273
ATTN: NSP-272

DEPARTMENT OF THE AIR FORCE

Aeronautical Systems Division
Air Force Systems Command
2 cy ATTN: ASD/ENFTV, O. Ward

Air Force Flight Dynamics Laboratory
ATTN: FXG

Air Force Geophysics Laboratory
ATTN: LY, C. Touart

Air Force Materials Laboratory
ATTN: LLM, T. Nicholas
ATTN: MBC, D. Schmidt
ATTN: MBE, G. Schmitt

Air Force Rocket Propulsion Laboratory
ATTN: LKCP, G. Beale

Headquarters
Air Force Systems Command
ATTN: SOSS
ATTN: XRTO

Air Force Technical Applications Center
ATTN: TF

Air Force Weapons Laboratory
Air Force Systems Command
ATTN: DYT
ATTN: DYV, A. Sharp
ATTN: SUL
ATTN: DYV
ATTN: ALO, L. James
ATTN: DYS
ATTN: Tech. Review
ATTN: HO, W. Minge
ATTN: DES, G. Ganong
2 cy ATTN: NTO

Arnold Engineering Development Center
Air Force Systems Command
ATTN: Library Documents

Deputy Chief of Staff
Operations Plans and Readiness
Department of the Air Force
ATTN: AFXOOSS

Deputy Chief of Staff
Research, Development & Acq.
Department of the Air Force
ATTN: AFRD
ATTN: AFRDQSM

DEPARTMENT OF THE AIR FORCE (Continued)

Foreign Technology Division
Air Force Systems Command
ATTN: TQTD
ATTN: SDBS, J. Pumphrey
ATTN: SDBQ

Space & Missile Systems Organization
Air Force Systems Command
ATTN: DYS

Space & Missile Systems Organization
Air Force Systems Command
ATTN: MNNR
ATTN: MNNH
ATTN: MNN

Space & Missile Systems Organization
Air Force Systems Command
ATTN: RSS
ATTN: RST
ATTN: RSSE

Strategic Air Command
Department of the Air Force
ATTN: XPQM
ATTN: XOBM
ATTN: XPFS
ATTN: DOXT

DEPARTMENT OF ENERGY

Department of Energy
ATTN: Document Control for OMA/RD&T

DEPARTMENT OF ENERGY CONTRACTOR

Sandia Laboratories
Livermore Laboratory
ATTN: Document Control for Library & Security Classification Division

DEPARTMENT OF DEFENSE CONTRACTORS

Acurex Corp.
ATTN: R. Rindal
ATTN: C. Nardo
ATTN: R. Kendall
ATTN: J. Huntington

Aeronautical Rsch. Assoc. of Princeton, Inc.
ATTN: C. Donaldson

Aerospace Corp.
ATTN: W. Barry
ATTN: R. Mortensen
ATTN: J. McClelland
ATTN: W. Mann
ATTN: H. Blaes
ATTN: R. Crolius
ATTN: R. Strickler
ATTN: D. Glenn

Analytic Services, Inc.
ATTN: J. Selig

Battelle Memorial Institute
ATTN: M. Vanderlind
ATTN: E. Unger
ATTN: R. Castle

DEPARTMENT OF DEFENSE CONTRACTORS (Continued)

AVCO Research & Systems Group
ATTN: J. Gilmore
ATTN: J. Stevens
ATTN: Document Control
ATTN: W. Reinecke
ATTN: W. Broding

Boeing Co.
ATTN: E. York
ATTN: B. Lempriere
ATTN: R. Dyrdahl
ATTN: R. Holmes

California Research & Technology, Inc.
ATTN: K. Kreyenhagen
ATTN: M. Rosenblatt

Calspan Corp.
ATTN: M. Holden

Effects Technology, Inc.
ATTN: R. Parisse
ATTN: R. Wengler
ATTN: J. Green

General Electric Co.
Re-Entry & Environmental Systems Div.
ATTN: P. Cline
ATTN: B. Maguire

General Electric Company-TEMPO
ATTN: B. Gambill
ATTN: DASIAC

General Research Corp.
ATTN: T. Stathacopoulos
ATTN: J. Ise, Jr.

Harold Rosenbaum Associates, Inc.
ATTN: G. Weber

Institute for Defense Analyses
ATTN: J. Bengston
ATTN: Classified Library

Kaman Sciences Corp.
ATTN: J. Hoffman
ATTN: J. Harper
ATTN: F. Shelton
ATTN: D. Sachs
ATTN: J. Keith
ATTN: T. Meagher

Lockheed Missiles & Space Co., Inc.
ATTN: R. Walz
ATTN: A. Collins

Lockheed Missiles and Space Co., Inc.
ATTN: F. Borgardt

McDonnell Douglass Corp.
ATTN: H. Berkowitz
ATTN: E. Fitzgerald
ATTN: H. Hurwicz
ATTN: P. Lewis, Jr.
ATTN: L. Cohen
ATTN: J. Garibotti
ATTN: P. Spangler
ATTN: D. Giedt

DEPARTMENT OF DEFENSE CONTRACTORS (Continued)

Meteorology Research, Inc.
ATTN: W. Green

Pacific-Sierra Research Corp.
ATTN: G. Lang

Particle Measuring Systems, Inc.
ATTN: R. Knollenberg
ATTN: S. Kunselman

Physics International Co.
ATTN: J. Shea

Prototype Development Associates, Inc.
ATTN: J. McDonald

R & D Associates
ATTN: P. Rausch
ATTN: H. Brode
ATTN: F. Field
ATTN: W. Graham, Jr.
ATTN: J. Carpenter
ATTN: C. MacDonald

Rand Corp.
ATTN: R. Rapp
ATTN: J. Mate

Science Applications, Inc.
ATTN: G. Ray
ATTN: D. Hove
ATTN: W. Yengst
ATTN: J. Warner
ATTN: O. Nance

Science Applications, Inc.
ATTN: G. Burghart

Science Applications, Inc.
ATTN: W. Seebaugh
ATTN: J. Cockayne
ATTN: C. Thomas

Science Applications, Inc.
ATTN: A. Martellucci

Southern Research Institute
ATTN: C. Pears

SRI International
ATTN: D. Curran
ATTN: G. Abrahamson
ATTN: H. Lindberg
ATTN: P. Dolan

System Planning Corp.
ATTN: F. Adelman

Systems, Science & Software, Inc.
ATTN: R. Duff
ATTN: G. Gurtman

Terra Tek, Inc.
ATTN: S. Green

DEPARTMENT OF DEFENSE CONTRACTORS (Continued)

TRW Defense & Space Sys. Group
ATTN: P. Dai
ATTN: R. Plebuch
ATTN: W. Wood
ATTN: T. Williams
ATTN: G. Arenguren
ATTN: P. Brandt
2 cy ATTN: D. Baer
2 cy ATTN: A. Zimmerman
2 cy ATTN: T. Mazzola
2 cy ATTN: I. Alber

DEPARTMENT OF DEFENSE CONTRACTORS (Continued)

TRW Defense & Space Sys. Group
ATTN: V. Blankenship
ATTN: W. Polich
ATTN: L. Berger
ATTN: E. Allen
ATTN: E. Wong